

People's Democratic Republic of Algeria
Ministry of Higher Education and Scientific Research
University M'Hamed BOUGARA – Boumerdes



Institute of Electrical and Electronic Engineering
Department of Power and Control

Final Year Project Report Presented in Partial Fulfilment of
the Requirements for the Degree of

MASTER

In Electrical and Electronic Engineering

Option: Control

Title:

**Modelling and Control of Mini Unmanned
Aerial Vehicles (UAV)**

Presented by:

- **DORBANE Sedik**
- **AIT SAID Azouaou**

Supervisor:

Dr. BOUSHAKI Razika

Registration Number:...../2019

Abstract

In this work, a detailed mathematical model for a Vertical Takeoff and Landing type Unmanned Aerial Vehicle known as the quadrotor is presented. The nonlinear dynamic model has been derived using Newton's and Euler's laws. Three control approaches were developed to control the altitude, attitude, heading and position of the quadrotor in space. The first approach is based on a linear Proportional-Integral-Derivative (PID) controller. The second developed controller is a nonlinear Back-stepping controller while the third one is a gain Grain-Scheduling based PID controller.

The Genetic Algorithm technique has been used to get an optimal tuning for the fore mentioned controllers (gains and parameters) and, hence, improving the dynamic response. Simulation based experiments were conducted using MATLAB to evaluate and compare between the three developed control techniques in terms of dynamic performance, stability and possible disturbances effect.

Dedication

I dedicate this modest work to my dear parents, my brothers and to all my family and friends.

Sedik

I dedicate this modest work to my dear parents, my brothers and to all my family and friends.

Azouaou

Acknowledgements

At the end of this work, we want to express our deep gratitude and appreciation to our supervisor Dr.Boushaki Razika, for the valuable suggestions, support and guidance. We are sincerely grateful to all the staff of the Institute of Electrical and Electronics Engineering of the University of M'Hamed Bougara- Boumerdes, Teachers and workers, especially the Control Department members, for the great help and support during the last five years. A special thanks to all of our teachers, we have learned a lot from you so thank you very much

Table of Contents

Abstract	I
Dedication.....	II
Acknowledgements	III
Table of Contents.....	IV
Table of Figures	VII
List of Tables.....	VIII
General Introduction.....	1
<i>Chapter I</i> System Modeling And Control	7
1-1 Kinematic Model	7
1-2 Dynamics Model	8
1-2-1 Rotational Equations of Motion	8
1-2-2 Translational Equations of Motion.....	12
1-3 Aerodynamic Effects	12
1-3-1 Drag Forces	13
1-3-2 Drag Moments	13
1-4 Rotor Dynamics	13
1-5 State Space Model.....	15
1-5-1 State Vector	15

1-5-2	Control Input Vector U.....	16
1-5-3	Rotational Equation of Motion.....	16
1-5-4	Translational Equation of Motion	17
1-5-5	State Space Representation.....	18
1-6	Control Strategies.....	19
1-6-1	Open Loop Simulation	19
1-6-2	Closed Loop Simulation.....	20
1-6-2-1	Altitude Control.....	20
1-6-2-2	Attitude and Heading Controller.....	20
1-6-2-3	Position Controller.....	21
Chapter II	PID Controller.....	23
2-1	PID Controller	23
2-2	Introduction to PID	23
2-3	Altitude Control	24
2-4	Attitude and Heading Control	24
2-4-1	Roll controller.....	24
2-4-2	Pitch Controller.....	24
2-4-3	Yaw Controller	25
2-5	Position Controller	25
2-6	PID Controller Simulation	26
2-6-1	PD Simulation without Disturbance	26
2-6-2	PD Simulation with Disturbance	28
Chapter III	Backstepping Controller	30
3-1	Backstepping Controller	30
3-2	Introduction to Backstepping.....	30
3-3	Attitude and Heading Controller	30
3-3-1	Roll Controller.....	30
3-3-2	Pitch Controller	32
3-3-3	Yaw Controller.....	33
3-4	Altitude Controller.....	34
3-5	Backstepping Controller Simulation	34
3-5-1	Backstepping Simulation without Disturbance	35
3-5-2	Backstepping Simulation with Disturbance	36

Chapter IV Gain Scheduling Based PD Controller.....	38
4-1 Gain Scheduling Based PD Controller	38
4-2 Introduction to Gain Scheduling.....	38
4-3 Gain Scheduling Based PD Controller Simulation	38
4-3-1 Altitude Controller.....	39
4-3-2 Attitude Controller.....	40
4-3-3 Heading Controller	41
4-4 Results Discussion.....	43
4-4-1 Proportional Derivative Control.....	43
4-4-2 Backstepping Control	43
4-4-3 Gain Scheduling PD Control	43
4-5 Comparison Between The Three Developed Controllers	44
General Conclusion	45
Bibliography:	

Table of Figures

Fig.1: Quadrotor notation for four motors.....	3
Fig.2: Coordinate system and Roll, Pitch, Yaw angles.	3
Fig.3: Generated motion of the quadrotor.	4
Fig. 1-1: Quadrotor reference frames.	7
Fig. 1-2: Forces and moments acting on the quadrotor.	11
Fig. 1-3: DC motor schematic diagram	14
Fig. 1-4: Open Loop Simulation.....	19
Fig. 1-5 : Block Diagram For Altitude Controller.....	20
Fig. 1-6: Block Diagram For Attitude and Heading Controller	21
Fig. 1-7: Position Controller Block Diagram (Complete System)	22
Fig. 2-1: PID Controller Block Diagram	23
Fig. 2-2: Global View of the Simulink Model of the System with PD Control	26
Fig. 2-3: PD Controller Simulation Response	27
Fig. 2-4: PD Controllers	28
Fig. 2-5: Trajectory Response	28
Fig. 2-6: PD Controller Simulation Response with Disturbance	29
Fig. 2-7: PD Controllers with Disturbance.....	29
Fig. 3-1: Global view of the Simulink Model of the System with backstepping Control	34
Fig. 3-2: Backstepping Controller Simulation Response	35
Fig. 3-3: Backstepping Controllers.....	36
Fig. 3-4: Backstepping Controller Simulation Response with Disturbance.....	37
Fig. 3-5: Backstepping Controllers with Disturbance	37
Fig. 4-1: Gain Scheduling Block Diagram	38
Fig. 4-3: Altitude Response.....	39
Fig. 4-3: Attitude Response.....	40
Fig. 4-4: Heading Response	41
Fig. 4-5: Controller Inputs.....	42
Fig 5 : Quadrotor Parameters and Constants.....	47

List of Tables

Table 2.1: Tuning PD parameters.....	26
Table 3.1: Tuning backstepping parameters.....	35
Table 4-1: Altitude Gain Scheduling Based PD controller Gains	39
Table 4-2: Attitude Gain Scheduling Based PD controller Gains.....	40
Table 4-3: Heading Gain Scheduling Based PD controller Gains	41

General Introduction

A quadrotor is a UAV (Unmanned Aerial Vehicle) with four rotors to control its motion in six degrees of freedom (6DOF). The pairs of rotors rotate in clockwise/counterclockwise direction [1]. For rolling and Pitching, Quadrotor tilts toward the direction of the slow spinning motor. Linear Motion is achieved by dividing the thrust into two directions which are done by roll and pitch angles. A quadrotor is difficult to be stabilized by human control. Hence, a controller must be designed for a balanced flight of the UAV [2]. Most of the practicing engineers and researchers have been using quadcopter for an incredible growth in applications and its simple mechanical design. The four motors or rotors affect position and attitude of quadrotor in space, hence there are four controllable variables used for balancing. With change in torque with respect to the one of the axes quadcopter inclination is achieved [3]. In this work, firstly kinematics is framed from a different perspective. This is followed by an effective use of Newton-Euler's method to derive equations with respect to the body frame of reference and inertial frame of reference. A mathematical model is derived, coordinate systems are defined and explained. By using those coordinate systems, relations between parameters defined in the earth coordinate system and in the body coordinate system are defined. Solutions have been obtained for important parameters such as linear acceleration, angular acceleration and torque. The developed mathematical framework is implemented in MATLAB.

1-Objectives and Motivation

This thesis work will focus on the modeling and control of a quadrotor. The reasons behind choosing the quadrotor is, in addition to its advantages, the research field is still facing some challenges in control because the high nonlinearity of the quadrotor and since it has six degrees of Freedom (DOF) but only four actuators, it is an underactuated system [4]. Underactuated systems are those having a less number of control inputs compared to the system's degrees of freedom. They are very difficult to control due to the nonlinear coupling between the actuators and the degrees of freedom [5]. Although the most common flight control algorithms found in literature are linear flight controllers, these controllers can only perform when the quadrotor is flying around hover, they suffer

from a huge performance degradation whenever the quadrotor leaves the nominal conditions or performs aggressive maneuvers [6].

The contributions of this work are: deriving an accurate and detailed mathematical model of the quadrotor UAV, developing linear and nonlinear control algorithms and applying those on the derived mathematical model in computer based simulations. The thesis will be concluded with a comparison between the developed control algorithms in terms of their dynamic performance and their ability to stabilize the system.

2-Unmanned Aerial Vehicles

The definition for UAVs varies from one literature to the other. For our purposes, UAVs are small aircrafts that are flown without a pilot. They can either be remotely operated by a human or they can be autonomous; autonomous vehicles are controlled by an onboard computer that can be preprogrammed to perform a specific task or a broad set of tasks. While in other literatures, UAVs may refer to powered or unpowered, tethered or untethered aerial vehicles [7]. The definition used in this thesis is based on that of the American Institute of Aeronautics and Astronautics [7]: An aircraft which is designed or modified not to carry a human pilot and is operated through electronic input initiated by the flight controller or by an on board autonomous flight management control system that does not require flight controller intervention. UAVs were mainly used in military application but recently they are being deployed in civil applications too [8].

3-The Quadrotor Concept

A quadrotor has four motors mounted at the ends of cross arm which are labelled as 1 through 4. The motor 1 & 3 rotate in counter clockwise whereas motor 2 & 4 rotates in clockwise direction or vice versa. The center of the body-fixed frame B is the center of mass and the origin, which is attached to the quadrotor. Rotor 1, 2, 3 and 4 produces upward thrust F_1 , F_2 , F_3 and F_4 respectively, and d is the length between the center of mass and center of rotor shown in Fig.1 [6].

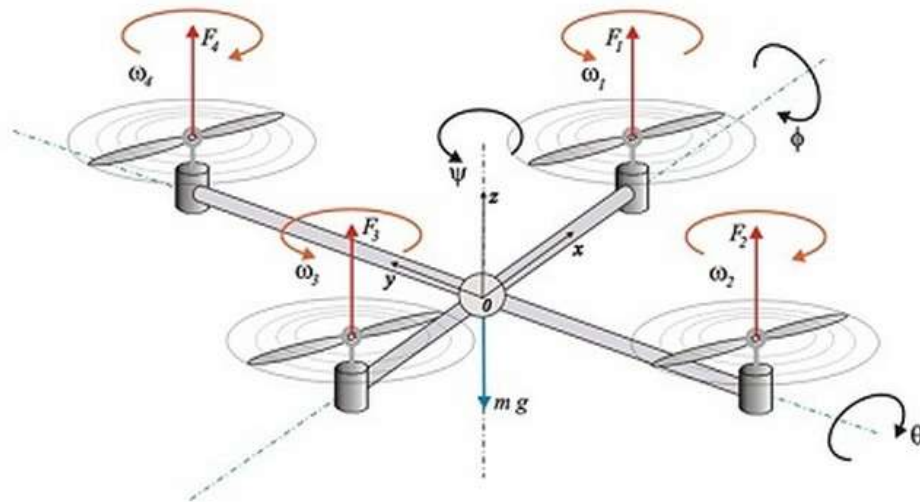


Fig.1: Quadrotor notation for four motors.

The quadrotor is a 6 DOF object, thus 6 variables are used to express its position in space (x, y, z, ϕ, θ and ψ). x, y and z represent the distances of the quadrotor's center of mass along the x, y and z axes respectively from an Earth fixed inertial frame. ϕ, θ and ψ are the three Euler angles representing the orientation of the quadrotor. ϕ is called the roll angle which is the angle about the x -axis, θ is the pitch angle about the y -axis, while ψ is the yaw angle about the z -axis. Fig.2 clearly explains the Euler Angles. The roll and pitch angles are usually called the attitude of the quadrotor, while the yaw angle is referred to as the heading of the quadrotor. For the linear motion, the distance from the ground is referred to as the altitude and the x and y position in space is often called the position of the quadrotor.

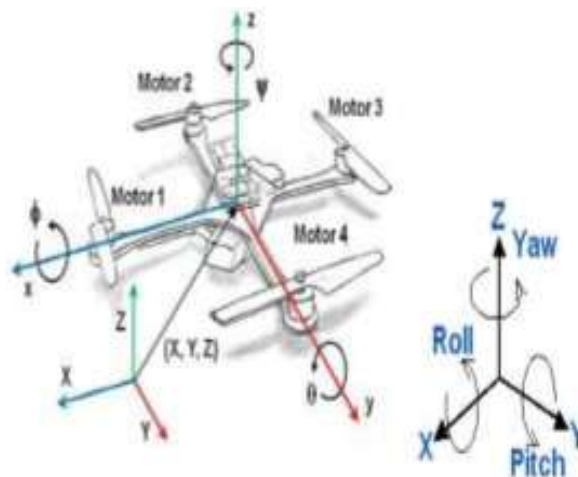


Fig.2: Coordinate system and Roll, Pitch, Yaw angles.

To generate vertical upwards motion, the speed of the four propellers is increased together whereas the speed is decreased to generate vertical downwards motion. To produce roll rotation coupled with motion along the y-axis, the second and fourth propellers speeds are changed while for the pitch rotation coupled with motion along the x-axis, it is the first and third propellers speeds that need to be changed.

One problem with the quadrotor configuration is that to produce yaw rotation, one need to have a difference in the opposite torque produced by each propeller pair. For instance, for a positive yaw rotation, the speed of the two clockwise turning rotors need to be increased while the speed of the two counterclockwise turning rotors need to be decreased [9, 10]. Fig.3 shows how different movements can be produced, note that a thicker arrow means a higher propeller speed.

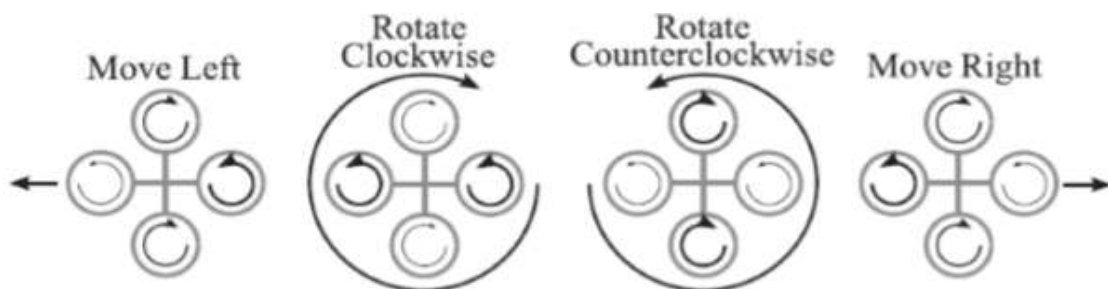


Fig.3: Generated motion of the quadrotor.

3-1 Advantages and Drawbacks of Quadrotor

Some advantages of the quadrotor over helicopters are that the rotor mechanics is simplified as it depends on four fixed pitch rotors unlike the variable pitch rotor in the helicopter, thus leading to easier manufacturing and maintenance. Moreover, the gyroscopic effects are reduced, due to the symmetry in the configuration, leading to simpler control.

The presence of four propellers providing four thrust forces shifted a fixed distance from the center of gravity instead of only one propeller centered in the middle as in the helicopters structure leads to a more stable stationary hovering in quadrotors [4].

More advantages are the vertical take-off and landing capabilities, better maneuverability and smaller size due to the absence of a tail [11], these capabilities make quadrotors useful in small area monitoring and buildings exploration [12].

Moreover, quadrotors have higher payload capacities due to the presence of four motors thus providing higher thrust [4].

On the other hand, quadrotors consume a lot of energy due to the presence of four separate propellers [12]. Also, they have a large size and heavier than some of their counterparts again to the fact that there are four separate propellers [12, 13].

4- Control

Several control techniques can be implemented and used to control a quadrotor. These techniques vary from the classical linear PID (Proportional-Integral-Derivative) to more complex nonlinear methods as the backstepping and SMC (Sliding Mode Controller) method. Although it is a linear controller used for the nonlinear multivariable quadrotor system, the PID or PD controller was found to be the most common control technique and it was proven successful in many literature [14].

4-1 Linear Flight Control Systems

They are typically based on PID, Linear Quadratic (LQ) or H_∞ algorithms and are the most common and conventional flight control systems.

Bouabdallah et al. proposed the usage of PID and LQ control methods to be applied on an indoor micro quadrotor, these two types of controllers performed comparably and were able to stabilize the quadrotor's attitude around its hover position when it undergoes little disturbances [14, 15]. Li and Li used the classical PID to control the position and orientation of a quadrotor and it was able to stabilize in a low speed wind environment [11]. Yang et al. used a self-tuning PID controller based on adaptive pole placement to control the attitude and heading of a quadrotor. Simulation showed that the proposed controller performed well with online tuning of the parameters [16].

Raffo et al. used an H_∞ controller to stabilize the rotational angles together with a Model Predictive Controller (MPC) to track the desired position [17]. The effect of wind and model uncertainties was added to the simulated model and it performed robustly with a zero steady-state error. H_∞ is a linear robust controller; robust controllers are those taking into account parametric uncertainty and unmodeled dynamics. It is reported that it is used for control of full-scaled helicopters [6].

Switched Dynamics and Gain Scheduling To use a linear controller to control a nonlinear system like a quadrotor, the nonlinearity of the system can be modelled as a collection of simplified linear models. This is the concept of gain scheduling and it is commonly used to design flight controllers. Gillula et al. divided the state space model of a STARMAC quadrotor to a set of simple hybrid modes and this approach enabled the quadrotor to carry out aerobatic maneuvers [18] [6] Also, Ataka et al. used gain scheduling on a linearized model of the quadrotor around some equilibrium points and tested the controllability and observability of the resulting system [19] Amoozgar et al. used a gain scheduled PID controller with the latter's parameters tuned using a fuzzy logic inference scheme to control a quadrotor. The system was tested under actuator fault conditions and compared with the performance of the conventional PID controller. The results showed a better performance for the gain scheduled PID controller [20] Sadeghzadeh et al. also use a gain scheduled PID controller applied to a quadrotor dropping a carried payload at a designated time. The algorithm was able to stabilize the system during the dropping operation [21]

4-2 Nonlinear Flight Control Systems

Because of the nonlinear nature dynamic of the quadrotor, the development of nonlinear control methods was necessary.

Backstepping is a recursive control algorithm that can be applied to both linear and nonlinear systems [6]. In a more recent paper, Bouabdallah and Siegwart proposed the use of backstepping nonlinear control method to control the quadrotor which performed better in presence of disturbances [12]. A Lyapunov stability theory based backstepping control realized by Madani and Benallegue to track desired values for the quadrotor's position and orientation. The system – quadrotor model- has been divided into 3 subsystems: underactuated, fully-actuated and propeller subsystems. Their proposed algorithm was able to stabilize the system under no disturbances [21]

Chapter I System Modeling And Control

In this chapter, a mathematical model for the quadrotor will be developed based on the Newton-Euler laws. The following assumptions have been made:

- The structure of the quadrotor is rigid and symmetrical.
- The center of mass of the quadrotor coincides with the body fixed frame origin.
- The propellers are rigid.
- The thrust and drag are proportional to the square of propeller's speed.

After the kinematics and dynamics models are derived, the aerodynamics effects acting on the quadrotor will be discussed together with the rotor dynamics of the actuators of the quadrotor. the chapter will be ended with the formulation of a state space model for the quadrotor system that will be used in the next chapter for modeling and testing.

1-1 Kinematic Model

In order to model the quadrotor, the coordinate frames that will be used has to be defined first. Fig.1-1 shows the Earth reference frame with N, E and D axes (pointing to the North, East and Downward respectively) and the body frame with x, y and z axes. The Earth frame is an inertial frame fixed on a specific place at ground level as its name implies. On the other hand, the body frame is at the center of the quadrotor body, with its x-axis pointing towards propeller 1, y-axis pointing towards propeller 2 and the z-axis is pointing to the ground.

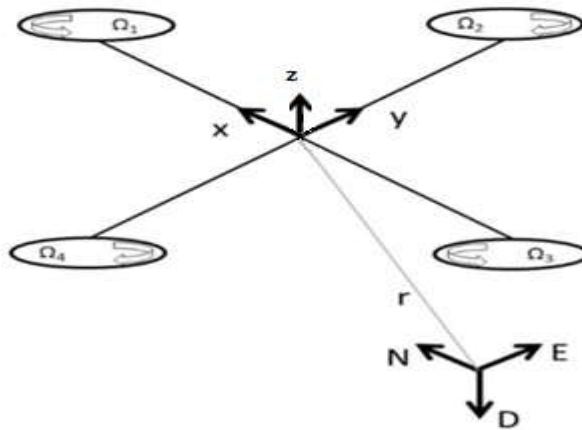


Fig.1-1: Quadrotor reference frames.

The distance between the Earth frame and the body frame describes the absolute position of the center of mass of the quadrotor $r = [x \ y \ z]^T$. The rotation R from the body frame to the inertial frame defines the orientation of the quadrotor. The orientation of the quadrotor is described using roll (ϕ), pitch (θ) and yaw (ψ) angles representing rotations about the X, Y and Z-axes respectively. Assuming the order of rotation to be roll, pitch then yaw, the rotation matrix R is then:

$$R = \begin{bmatrix} \cos(\theta) \cos(\psi) & \cos(\psi) \sin(\theta) \sin(\phi) - \cos(\phi) \sin(\psi) & \cos(\phi) \sin(\theta) \cos(\psi) + \sin(\phi) \sin(\psi) \\ \cos(\theta) \sin(\psi) & \sin(\phi) \sin(\theta) \sin(\psi) + \cos(\theta) \cos(\psi) & \cos(\phi) \sin(\theta) \sin(\psi) - \sin(\theta) \cos(\psi) \\ -\sin(\theta) & \sin(\phi) \cos(\theta) & \cos(\phi) \cos(\theta) \end{bmatrix} \quad (1.1)$$

The rotation matrix R will be used to derive the dynamic model of the quadrotor because of the fact that some states are measured in the body frame while some other are measured in the inertial frame. Hence, a transformation between the two frames is needed.

To relate the Euler rates $\dot{\eta} = [\dot{\phi} \ \dot{\theta} \ \dot{\psi}]^T$ that are measured in the inertial frame and angular body rates $= [p \ q \ r]^T$, a transformation is needed as follows:

$$\omega = R_r \dot{\eta} \quad (1.2)$$

Where

$$R_r = \begin{bmatrix} 1 & 0 & -\sin(\theta) \\ 0 & \cos(\phi) & \sin(\phi) \cos(\theta) \\ 0 & -\sin(\phi) & \cos(\phi) \cos(\theta) \end{bmatrix}$$

Around the hover, small angle assumption can be made where $\cos(\phi) \approx 1$, $\cos(\theta) \approx 1$ and $\sin(\phi) \approx 0$, $\sin(\theta) \approx 0$. This leads to the identity matrix I .

1-2 Dynamics Model

The quadrotors motion can be divided into two subsystems; a rotational subsystem with roll, pitch and yaw angles and a translational subsystem with altitude and x & y position. The rotational subsystem is fully actuated while the translational one is underactuated [22].

1-2-1 Rotational Equations of Motion

Applying Newton-Euler method in the body frame, the rotational equations of motion are derived with the following formalism:

$$J\dot{\omega} + \omega \times J\omega + M_G = M_B \quad (1.3)$$

Where

J is the quadrotor's diagonal inertia matrix.

ω is the angular body rates.

M_G is the gyroscopic moments due to rotors' inertia.

M_B are the moments acting on the quadrotor in the body frame.

$J\dot{\omega}$ and $\omega \times J\omega$ in equation 1.3 represent the rate of change of angular momentum in the body frame. M_G represent the gyroscopic moments due to the rotor's inertia J_r .

M_G are defined to be $\omega \times [0 \ 0 \ J_r\Omega_r]^T$, where J_r is the rotors' inertia and Ω_r the rotors' relative speed ($\Omega_r = -\Omega_1 + \Omega_2 - \Omega_3 + \Omega_4$) [19].

Equation 1.3 can be written as:

$$J\dot{\omega} + \omega \times J\omega + \omega \times [0 \ 0 \ J_r\Omega_r]^T = M_B \quad (1.4)$$

Writing the rotational equations of motion in the body frame makes the inertia matrix independent of time. For this reason, they have not been written in the inertial frame.

Inertia Matrix

The inertia matrix is given by:

$$I = \begin{bmatrix} I_{xx} & 0 & 0 \\ 0 & I_{yy} & 0 \\ 0 & 0 & I_{zz} \end{bmatrix} \quad (1.5)$$

Due to the symmetry of the quadrotor, the off-diagonal, which are the product of inertia, elements are zero.

I_{xx} , I_{yy} and I_{zz} are the area moments of inertia about the principle axes in the body frame.

Gyroscopic Moments

The gyroscopic moment of a rotor is a physical effect in which gyroscopic torques or moments attempt to align the spin axis of the rotor along the inertial z-axis [23].

Moments Acting on the Quadrotor

To define the last term of equation (1.4), M_B , two physical effects have to be defined first. These physical effects are the aerodynamic forces and moments produced by a rotor.

The rotation generates a force called the aerodynamic force and there is a generated moment called the aerodynamic moment.

Equations (1.6) and (1.7) show the aerodynamic force F_i and the aerodynamic moment M_i respectively produced by the i^{th} rotor [8].

$$F_i = \frac{1}{2} \rho A C_T r^2 \Omega_i^2 \quad (1.6)$$

$$M_i = \frac{1}{2} \rho A C_D r^2 \Omega_i^2 \quad (1.7)$$

Where

ρ is the air density

A blade area

C_D, C_T aerodynamic coefficients

r the radius of blade

Ω_i angular velocity of rotor i

It can be seen that the aerodynamic force and moment depend on the geometry of propeller and the air density. Since the altitude is usually limited, the air density can be considered as constant. Thus, simplifying the equations (1.6) and (1.7) to:

$$F_i = K_f \Omega_i^2 \quad (1.8)$$

$$M_i = K_M \Omega_i^2 \quad (1.9)$$

K_f and K_M are aerodynamic force and moment constants respectively. They can be determined experimentally for each propeller type.

Identifying the forces and moments generated by the propellers helps the study the moments M_B acting on the quadrotor. Each rotor causes an upward thrust force F_i and generated a moment M_i with opposite direction to the rotation of the corresponding rotor i . Forces and moments acting on the quadrotor are shown in Fig.1-2.

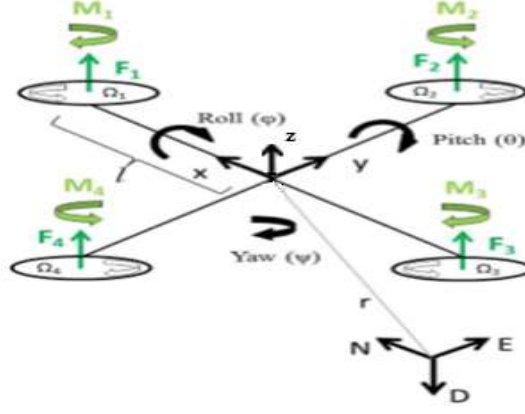


Fig.1-2: Forces and moments acting on the quadrotor.

The moments about the body frame's x-axis; by using the right-hand rule in association with the axes of the body frame, F_2 multiplied by the moment arm l generates a negative moment about the y-axis, while in the same manner, F_4 generates a positive moment. Thus the total moment about the x-axis is:

$$\begin{aligned} M_x &= -F_2 l + F_4 l = -(K_f \Omega_2^2) l + (K_f \Omega_4^2) l \\ M_x &= l K_f (-\Omega_2^2 + \Omega_4^2) \end{aligned} \quad (1.10)$$

Using the same method, the moments about the body frame's y-axis are:

$$M_y = l K_f (\Omega_1^2 - \Omega_3^2) \quad (1.11)$$

The moments about the body frame's z-axis are obtained using the right hand rule. Since the thrust of the motor does not cause a moment, the moment is caused by the rotors' rotation as per equation (1.7).

$$\begin{aligned} M_z &= -M_1 + M_2 - M_3 + M_4 \\ &= -(K_M \Omega_1^2) + (K_M \Omega_2^2) - (K_M \Omega_3^2) + (K_M \Omega_4^2) \\ &= K_M (-\Omega_1^2 + \Omega_2^2 - \Omega_3^2 + \Omega_4^2) \end{aligned} \quad (1.12)$$

Combining equations (1.10), (1.11) and (1.12):

$$M_B = \begin{bmatrix} K_f (-\Omega_2^2 + \Omega_4^2) \\ K_f (\Omega_1^2 - \Omega_3^2) \\ K_M (-\Omega_1^2 + \Omega_2^2 - \Omega_3^2 + \Omega_4^2) \end{bmatrix} \quad (1.13)$$

Where l is the moment arm (the distance between the axis of rotation of each rotor to the origin of the body reference frame which coincide with the center of the quadrotor).

1-2-2 Translational Equations of Motion

The Newton's second law is used to derive the translational equations of motion in the earth frame [22].

$$m\ddot{r} = \begin{bmatrix} 0 \\ 0 \\ -mg \end{bmatrix} + RF_B \quad (1.14)$$

Where

$r = [x \ y \ z]^T$ quadrotor's distance from the inertial frame.

m quadrotor's mass

g gravitational acceleration $g = 9.81 \text{ m/s}^2$

F_B nongravitational forces acting on the quadrotor.

Nongravitational forces acting on the quadrotor

When the quadrotor is in a horizontal orientation (i.e. it is not rolling or pitching), the only nongravitational force acting on it is the thrust produced by the rotation of the propellers defined by Equation (1.8). Thus, the nongravitational forces acting on the quadrotor are:

$$F_B = \begin{bmatrix} 0 \\ 0 \\ K_f(\Omega_1^2 + \Omega_2^2 + \Omega_3^2 + \Omega_4^2) \end{bmatrix} \quad (1.15)$$

The first two rows of the force vector are zeros as there is no forces in the X and Y directions, the last row is simply an addition of the thrust forces produced by the four propellers. The negative sign is due to the fact that the thrust is upwards while the positive z-axis in the body framed is pointing downwards.

F_B is multiplied by the rotation matrix R to transform the thrust forces of the rotors from the body frame to the inertial frame, so that the equation can be applied in any orientation of the quadrotor.

1-3 Aerodynamic Effects

In order to have an accurate and realistic model, the aerodynamic effects must not be neglected and should be included. There are namely two types of aerodynamic effects, drag forces and drag moments [24].

1-3-1 Drag Forces

When the quadrotor moves in air, a frictional force resisting the motion is produced, the drag force. It is directly proportional to the velocity of the traveling body. It is approximated by:

$$F_a = K_t \dot{r} \quad (1.16)$$

K_t is a constant matrix called the aerodynamic translation coefficient matrix and \dot{r} is the derivative of the position vector r .

Thus, equation (1.14) should be rewritten to be:

$$m\ddot{r} = \begin{bmatrix} 0 \\ 0 \\ -mg \end{bmatrix} + RF_B - F_a \quad (1.17)$$

1-3-2 Drag Moments

As the drag force, due to the air friction there is a drag moment acting on the quadrotor approximated by:

$$M_a = K_r \dot{\eta} \quad (1.18)$$

K_r is a constant matrix called the aerodynamic rotation coefficient matrix and $\dot{\eta}$ is the Euler rate. Equation (1.4) is written as:

$$J\dot{\omega} + \omega \times J\omega + \omega \times [0 \quad 0 \quad J_r\Omega_r]^T = M_B - M_a \quad (1.19)$$

1-4 Rotor Dynamics

Brushless DC motors are the mostly used in quadrotor providing high torque and less friction. In this derivation the motors are assumed to be nongearred with rigid mechanical coupling between the motors and propellers. In steady state, the dynamics of a brushless DC motor is the same as the conventional DC motor and it is shown in Fig.1-3.

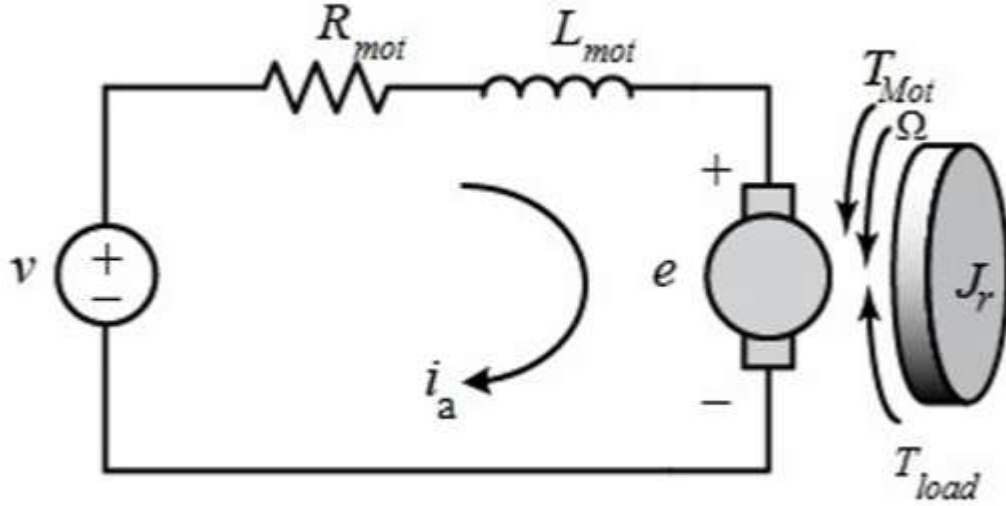


Fig.1-3: DC motor schematic diagram

Using Kirchhoff's Voltage Law (KVL)

$$v = R_{mot}i_a + L_{mot} \frac{di_a}{dt} + K_{mot}\Omega_i \quad (1.20)$$

R_{mot} and L_{mot} are the i^{th} motor's resistance and inductance respectively. i_a is the armature current and v is the input voltage while $K_{mot}\Omega$ is the generated emf e , with K_{mot} the motor torque constant .

Since the quadrotor relies on small motors, their inductance is very small and can be neglected leading to:

$$v = R_{mot}i_a + K_{mot}\Omega_i \quad (1.21)$$

And

$$i_a = \frac{v - K_{mot}\Omega_i}{R_{mot}} \quad (1.22)$$

The mechanical derivation is then:

$$J_r\dot{\Omega}_i = T_{mot} - T_{load} \quad (1.23)$$

$T_{mot} = K_e i_a$ is the torque produced by the motor where K_e is the motor's electric constant and for small motors it is approximated to be $K_{mot} \cdot T_{load} = K_M \Omega^2$ is the load torque generated by from the propeller system as per equation (1.7).

Substituting T_{mot} and T_{load} with equation (1.22) yields to

$$J_r \dot{\Omega}_i = K_{mot} \frac{v - K_{mot} \Omega_i}{R_{mot}} - K_M \Omega_i^2 \quad (1.24)$$

Which can be simplified to

$$v = \frac{R_{mot}}{K_{mot}} J_r \dot{\Omega}_i + K_{mot} \Omega_i + K_M R_{mot} \Omega_i^2 \quad (1.25)$$

The rotor dynamics can be approximated to a first order lag transfer function with its parameters (gain and time constant) identified experimentally by using a system identification tool (e.g. MATLAB's System Identification Toolbox). The transfer function maps the desired propeller's speed to the actual speed [13]. The first order lag transfer function was identified to be:

$$G(s) = \frac{\text{Actual rotor speed}}{\text{Commanded rotor speed}} = \frac{0.936}{0.178s + 1} \quad (1.26)$$

Brushless DC motor typically have their own embedded controllers and they work with a Pulse Width Modulated (PWM) signal. The voltage supplied to the brushless DC motor is directly proportional to the RPM of their rotation, the relationship can be found by a black box identification process for the motor and propeller pair. The constant of proportionality of this linear relationship appears as a gain in the transfer function in (1.26).

1-5 State Space Model

The acquired mathematical models will be formulated to a state space model to make control problem easier.

1-5-1 State Vector

Defining the state vector of the quadrotor to be:

$$X = [x_1 \ x_2 \ x_3 \ x_4 \ x_5 \ x_6 \ x_7 \ x_8 \ x_9 \ x_{10} \ x_{11} \ x_{12}]^T \quad (1.27)$$

This is mapped to the degrees of freedom of the quadrotor in the following:

$$X = [\phi \ \dot{\phi} \ \theta \ \dot{\theta} \ \psi \ \dot{\psi} \ z \ \dot{z} \ x \ \dot{x} \ y \ \dot{y}]^T \quad (1.28)$$

The state vector defines the position of the quadrotor in space and its angular and linear velocity.

1-5-2 Control Input Vector U

The control vector U consisting of the control inputs U_1 through U_4 is defined to be:

$$U = [U_1 \ U_2 \ U_3 \ U_4] \quad (1.29)$$

Where

$$U_1 = K_f(\Omega_1^2 + \Omega_2^2 + \Omega_3^2 + \Omega_4^2) \quad (1.30)$$

$$U_2 = K_f(-\Omega_2^2 + \Omega_4^2) \quad (1.31)$$

$$U_3 = K_f(\Omega_1^2 - \Omega_3^2) \quad (1.32)$$

$$U_4 = K_M(-\Omega_1^2 + \Omega_2^2 - \Omega_3^2 + \Omega_4^2) \quad (1.33)$$

In matrix form:

$$\begin{bmatrix} U_1 \\ U_2 \\ U_3 \\ U_4 \end{bmatrix} = \begin{bmatrix} K_f & K_f & K_f & K_f \\ 0 & -K_f & 0 & -K_f \\ K_f & 0 & -K_f & 0 \\ -K_M & K_M & -K_M & K_M \end{bmatrix} \begin{bmatrix} \Omega_1^2 \\ \Omega_2^2 \\ \Omega_3^2 \\ \Omega_4^2 \end{bmatrix} \quad (1.34)$$

U_1 is the resulting upwards force of the four rotors which is responsible for the altitude of the quadrotor and its rate of change (z, \dot{z}). U_2 is the difference in thrust between rotors 2 and 4 which is responsible for the roll rotation and its rate of change ($\phi, \dot{\phi}$). U_3 on the other hand, represents the difference in thrust between rotors 1 and 3 thus generating the pitch rotation and its rate of change ($\theta, \dot{\theta}$). Finally, U_4 is the difference in torque between the two clockwise turning rotors and the two counterclockwise turning rotors generating the yaw rotation and ultimately its rate of change ($\psi, \dot{\psi}$).

1-5-3 Rotational Equation of Motion

The equation of the total moments acting on the quadrotor becomes, by substituting equations (1.30) through (1.33) in equation (1.13):

$$M_B = l \begin{bmatrix} U_2 \\ U_3 \\ U_4 \end{bmatrix} \quad (1.35)$$

Substituting this in rotational equation of motion (3.4), and by expanding, the following is derived:

$$\begin{bmatrix} I_{xx}\ddot{\phi} \\ I_{yy}\ddot{\theta} \\ I_{zz}\ddot{\psi} \end{bmatrix} + \begin{bmatrix} \dot{\theta}I_{zz}\dot{\psi} - \dot{\psi}I_{zz}\dot{\theta} \\ \dot{\psi}I_{xx}\dot{\phi} - \dot{\phi}I_{zz}\dot{\psi} \\ \dot{\phi}I_{yy}\dot{\theta} - \dot{\theta}I_{zz}\dot{\phi} \end{bmatrix} + \begin{bmatrix} \dot{\theta}J_r\Omega_r \\ -\dot{\phi}J_r\Omega_r \\ 0 \end{bmatrix} = l \begin{bmatrix} U_2 \\ U_3 \\ U_4 \end{bmatrix} \quad (1.36)$$

Rewriting to have the angular acceleration in term of the other variables:

$$\ddot{\phi} = \frac{l}{I_{xx}}U_2 - \frac{J_r}{I_{xx}}\dot{\theta}\Omega_r + \frac{I_{yy}}{I_{xx}}\dot{\psi}\dot{\theta} - \frac{I_{zz}}{I_{xx}}\dot{\theta}\dot{\psi} \quad (1.37)$$

$$\ddot{\theta} = \frac{l}{I_{yy}}U_3 - \frac{J_r}{I_{yy}}\dot{\phi}\Omega_r + \frac{I_{zz}}{I_{yy}}\dot{\phi}\dot{\psi} - \frac{I_{xx}}{I_{yy}}\dot{\psi}\dot{\phi} \quad (1.38)$$

$$\ddot{\psi} = \frac{l}{I_{zz}}U_4 + \frac{I_{xx}}{I_{zz}}\dot{\theta}\dot{\phi} - \frac{I_{yy}}{I_{zz}}\dot{\phi}\dot{\theta} \quad (1.39)$$

By defining the following constants:

$$\begin{aligned} a_1 &= \frac{I_{yy} - I_{zz}}{I_{xx}} \\ a_2 &= \frac{J_r}{I_{xx}} & b_1 &= \frac{l}{I_{xx}} \\ a_3 &= \frac{I_{zz} - I_{xx}}{I_{yy}} & b_2 &= \frac{l}{I_{yy}} \\ a_4 &= \frac{J_r}{I_{yy}} & b_3 &= \frac{l}{I_{zz}} \\ a_5 &= \frac{I_{xx} - I_{yy}}{I_{zz}} \end{aligned}$$

Using the definitions above, equations (1.37) through (1.39) can be written as:

$$\ddot{\phi} = b_1U_2 - a_2x_4\Omega_r + a_1x_4x_6 \quad (1.40)$$

$$\ddot{\theta} = b_2U_3 + a_4x_2\Omega_r + a_3x_2x_6 \quad (1.41)$$

$$\ddot{\psi} = b_3U_4 + a_5x_2x_4 \quad (1.42)$$

1-5-4 Translational Equation of Motion

By substituting equations (1.30) through (1.33) in equation (1.15), the equation of the total moments acting on the quadrotor is:

$$F_B = [0 \quad 0 \quad U_1]^T \quad (1.43)$$

Substituting in the equation (3.14) and expanding, the following is got:

$$m \begin{bmatrix} \ddot{x} \\ \ddot{y} \\ \ddot{z} \end{bmatrix} = \begin{bmatrix} 0 \\ 0 \\ -mg \end{bmatrix} + \begin{bmatrix} (\sin(\phi)\sin(\psi) + \cos(\phi)\cos(\psi)\sin(\theta))U_1 \\ (\cos(\phi)\sin(\psi)\sin(\theta) - \cos(\psi)\sin(\phi))U_1 \\ \cos(\phi)\cos(\theta)U_1 \end{bmatrix} \quad (1.44)$$

Rewriting in term of the state variable X

$$\ddot{x} = \frac{U_1}{m} (\sin(x_1) \sin(x_5) + \cos(x_1) \cos(x_5) \sin(x_3)) \quad (1.45)$$

$$\ddot{y} = \frac{U_1}{m} (\cos(x_1) \sin(x_5) \sin(x_3) - \cos(x_5) \sin(x_1)) \quad (1.46)$$

$$\ddot{z} = -g + \frac{U_1}{m} (\cos(x_1) \cos(x_3)) \quad (1.47)$$

It can clearly be seen that the translational subsystem is underactuated as it depends on both the translational variables and rotational ones.

1-5-5 State Space Representation

Using the equations of the rotational angular acceleration. Equations (1.40) to (1.42), and those of translation, Equations (1.45) to (1.47), the complete mathematical model of the quadrotor can be written in a state space representation as follows,

$$\begin{aligned} \dot{x}_1 &= \dot{\phi} = x_2 \\ \dot{x}_2 &= \ddot{\phi} = x_4 x_6 a_1 - x_4 \Omega_r a_2 + b_1 U_2 \\ \dot{x}_3 &= \dot{\theta} = x_4 \\ \dot{x}_4 &= \ddot{\theta} = x_2 x_6 a_3 + x_2 \Omega_r a_4 + b_2 U_3 \\ \dot{x}_5 &= \dot{\psi} = x_6 \\ \dot{x}_6 &= \ddot{\psi} = x_2 x_4 a_5 + b_3 U_4 \\ \dot{x}_7 &= \dot{z} = x_8 \\ \dot{x}_8 &= \ddot{z} = -g + \frac{U_1}{m} (\cos x_1 \cos x_2) \\ \dot{x}_9 &= \dot{x} = x_{10} \\ \dot{x}_{10} &= \ddot{x} = \frac{U_1}{m} (\sin x_1 \sin x_5 + \cos x_1 \sin x_3 \cos x_5) \\ \dot{x}_{11} &= \dot{y} = x_{12} \\ \dot{x}_{12} &= \ddot{y} = \frac{U_1}{m} (-\sin x_1 \cos x_5 + \cos x_1 \sin x_3 \sin x_5) \end{aligned} \quad (1.48)$$

1-6 Control Strategies

In this thesis, the formulated quadrotor model will be used in open-loop simulations and with a controllers linear (PID, Gain scheduling) and nonlinear (Backstepping).The parameters and the gain of these controllers will be tuned using Genetic Algorithm.

1-6-1 Open Loop Simulation

The quadrotor's parameters were taken from Bouabdallah's PhD thesis which is based on the OS4 hardware [25]. The formulated quadrotor model will be used in open-loop simulations to verify the mathematical model, an open loop simulation was carried out using MATLAB/Simulink.

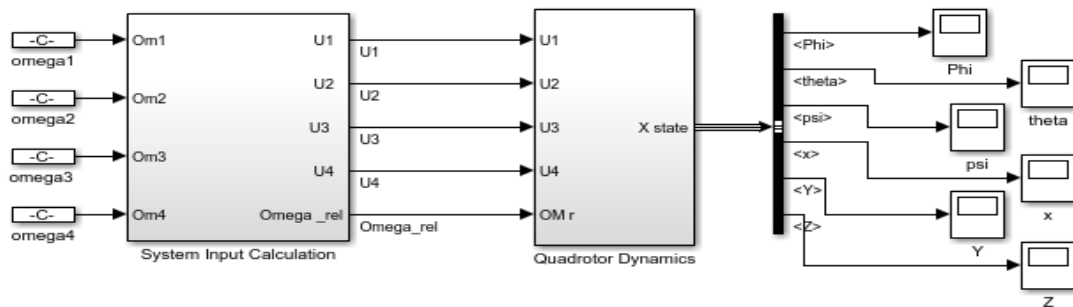


Fig. 1-4: Open Loop Simulation

The hovering point of the quadrotor was calculated from this equation.

$$mg = 4F_i$$

$$mg = 4(K_f \Omega_{ih}^2) \quad (1.49)$$

Where Ω_{ih} are the hover angular velocity of rotor i .

It is assumed that the only force acting on the quadrotor are Ω_i and the gravitational acceleration. When Ω_i have the same values all the state variables (x, y, ϕ, θ, ψ) are zero the only change was in the altitude z . It was observed there cases when Ω_i less then the hovering angular velocity the altitude go downwards, at the hovering point $z = 0$ by increasing Ω_i over the hovering angular velocity the altitude go upwards. Varying the angular velocity of the 4 motors produced the roll, pith or yaw motion.

Roll: when Ω_1 and Ω_3 have the same values but Ω_2 and Ω_4 are different from each other.

Pitch: when Ω_2 and Ω_4 have the same values but Ω_1 and Ω_3 are different from each other.

Yaw: when Ω_1 and Ω_3 have the same values but Ω_2 and Ω_4 have another same values.

Rotor dynamics are included in the ‘control input calculation’ block as the first order lag transfer function shown in equation (1.26).

1-6-2 Closed Loop Simulation

After testing the developed model in the open loop simulation, the simulation is then extended to include altitude, attitude, heading, and position controllers.

1-6-2-1 Altitude Control

The altitude control takes an error signal e as an input which is the difference between the desired altitude Z_d and the altitude Z and produced a control signal U_1 , as shown in the block diagram in Figure 2-1.

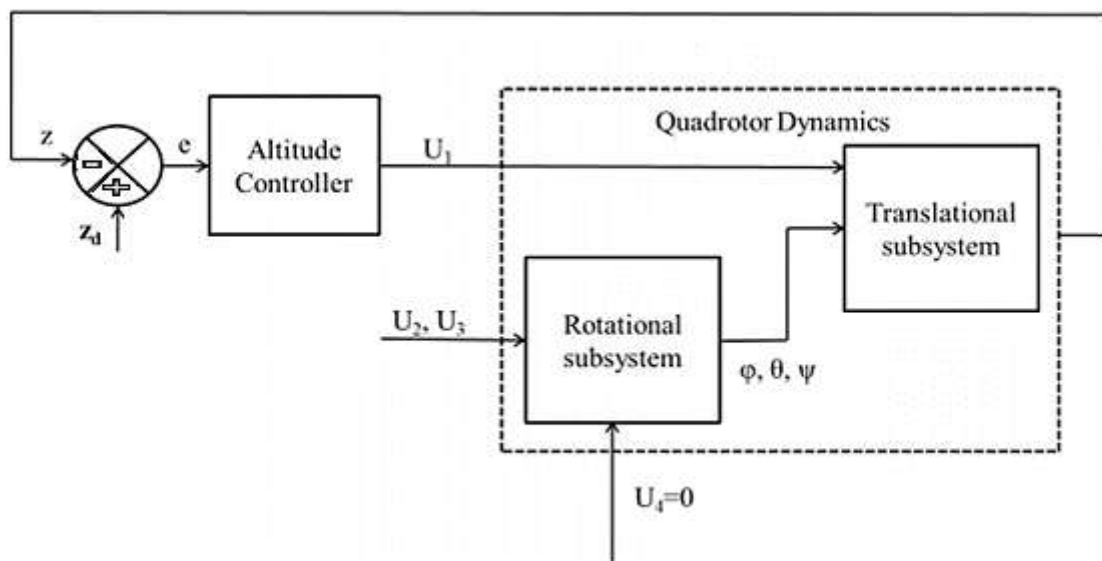


Fig. 1-5 : Block Diagram For Altitude Controller

1-6-2-2 Attitude and Heading Controller

The attitude and heading controller take as an input an error signal e which is the difference between the desired roll ϕ_d , pitch θ_d and yaw ψ_d and their actual values ϕ, θ, ψ . The attitude and heading controller produces the output signals U_2, U_3 and U_4 , as shown in Figure 2-2.

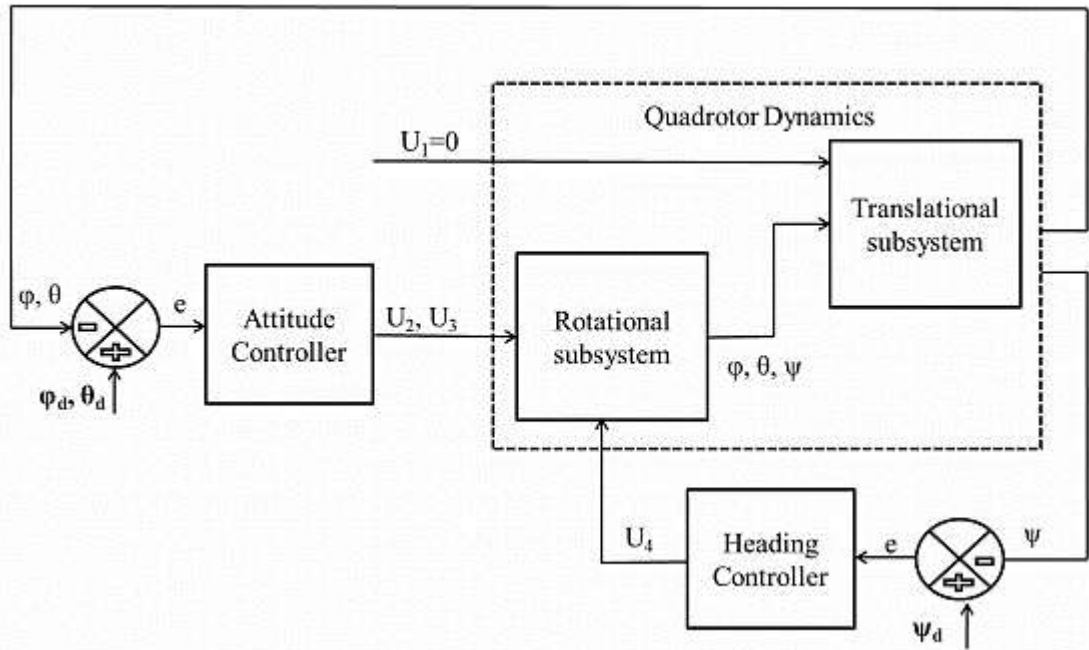


Fig. 1-6: Block Diagram For Attitude and Heading Controller

1-6-2-3 Position Controller

The x and y position can be controlled through the roll and pitch angles, because the system is not decoupled and cannot be directly controlled using one of the four control laws U_1 through U_4 .

Since the quadrotor is operating around the hover, which means small values of roll and pitch angles ϕ and θ we can use the small angles assumption ($\sin \phi_d \equiv \phi_d$, $\sin \theta_d \equiv \theta_d$, and $\cos \phi_d = \cos \theta_d = 1$) to simplify the equations (3.45) (3.46).

$$\ddot{x} = \frac{U_1}{m} (\phi_d \sin(\psi) + \theta_d \cos(\psi)) \quad (1.50)$$

$$\ddot{y} = \frac{U_1}{m} (\theta_d \sin(\psi) - \phi_d \cos(\psi)) \quad (1.51)$$

The calculated ϕ_d and θ_d have to be limited to the range between -20° and 20° to fulfill the small angle assumption used in the derivation and this can be done via a saturation function in the simulation.

The closed loop simulation for the altitude and attitude controllers is further enhanced to include the position controller as shown in the block diagram Figure 2-3.

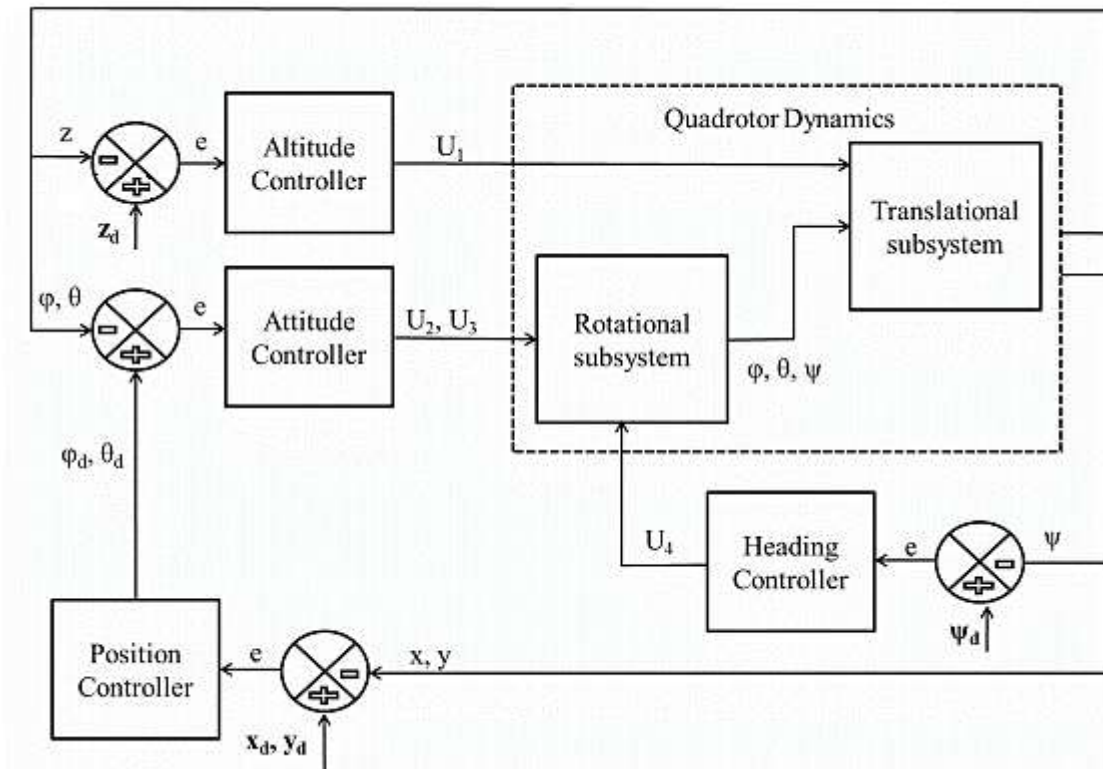


Fig. 1-7: Position Controller Block Diagram (Complete System)

Chapter II PID Controller

2-1 PID Controller

After the mathematical model of the quadrotor along with its open loop simulation are verified, a PID controller was developed. The PID controller generates the desired control inputs for the quadrotor. A PD control is used instead of PID for the sake of simplicity. The block diagram for a PID controller is shown in Figure 2.1.

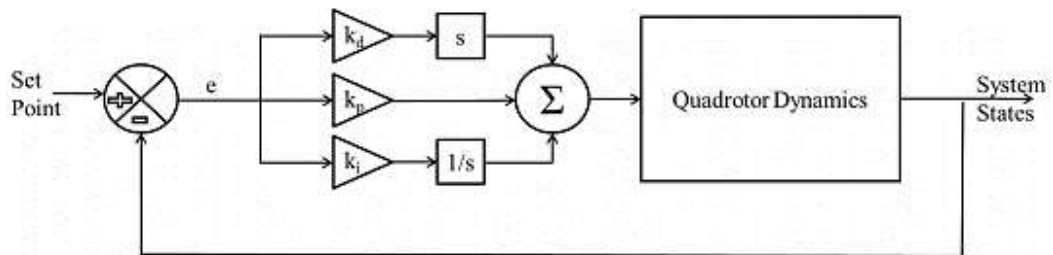


Fig. 2-1: PID Controller Block Diagram

2-2 Introduction to PID

The Proportional Integral Derivate Control is one of the simplest linear control laws. It is very simple and computationally efficient. It can be easily implemented in real time systems using microcontrollers. The mathematical simplicity and ease of understanding makes it one of the most used control laws in Aerial Robotics.

A PID controller is a generic control loop feedback mechanism. It measures a system output and checks it against a desired set point; it then adjusts the system input such that its output stays as close as possible to the desired set point. As its name suggests, the PID controller contains three constant parameters: the Proportional “P”, the Integral “I” and the Derivative “D”. Each of these three parameters has a different impact on the controller output:

- The proportional component depends only on the computed error term between the System’s output and the set point. In other words, “P” depends on the present error.
- The integral component sums the error term over time. The result is that even a small error term will cause the integral component to increase slowly. The integral response will continually increase over time unless the error is zero. In other words, “I” depends on the accumulation of past errors.

- The derivative component causes the controller output to decrease if the system's output is increasing rapidly. The derivative response is proportional to the rate of change of the process variable

2-3 Altitude Control

A PID controller is developed to control the altitude of the quadrotor, it is generate the control input U_1 which is responsible for the altitude of the quadrotor as per Equation (1.30). The derived control law is as follows:

$$U_1 = k_p(z_d - z) + k_d(\dot{z}_d - \dot{z}) + k_i \int (z_d - z)dt \quad (2.1)$$

Where

k_p Proportional gain

z_d Desired altitude

k_d Derivative gain

\dot{z}_d Desired altitude rate of change

k_i Integral gain

2-4 Attitude and Heading Control

2-4-1 Roll controller

Similar to the pitch and roll controllers, a yaw controller was developed to generate the control input U_4 based on the following control law:

$$U_2 = k_p(\phi_d - \phi) + k_d(\dot{\phi}_d - \dot{\phi}) + k_i \int (\phi_d - \phi)dt \quad (2.2)$$

Where

k_p Proportional gain

ϕ_d Desired roll angle

k_d Derivative gain

$\dot{\phi}_d$ Desired roll angle rate of change

k_i Integral gain

2-4-2 Pitch Controller

Another PID controller is developed to control the roll angle θ of the quadrotor. The derived control law generates the input U_3 that controls the roll angle as follows:

$$U_3 = k_p(\theta_d - \theta) + k_d(\dot{\theta}_d - \dot{\theta}) + k_i \int (\theta_d - \theta)dt \quad (2.3)$$

Where

k_p Proportional gain
 θ_d Desired pitch angle
 k_d Derivative gain
 $\dot{\theta}_d$ Desired pitch angle rate of change
 k_i Integral gain

2-4-3 Yaw Controller

A PID controller is developed to control the pitch angle ψ of the quadrotor. The derived control law generates the input U_2 that controls the pitch angle as follows:

$$U_4 = k_p(\psi_d - \psi) + k_d(\dot{\psi}_d - \dot{\psi}) + k_i \int (\psi_d - \psi) dt \quad (2.4)$$

Where

k_p Proportional gain
 ψ_d Desired yaw angle
 k_d Derivative gain
 $\dot{\psi}_d$ Desired yaw angle rate of change
 k_i Integral gain

2-5 Position Controller

After acquiring stable controllers for the altitude and the attitude of the quadrotor, a complete position controller is developed. PID controllers are used to calculate the desired accelerations x and y .

$$\ddot{x}_d = k_p(x_d - x) + k_d(\dot{x}_d - \dot{x}) + k_i \int (x_d - x) dt \quad (2.5)$$

$$\ddot{y}_d = k_p(y_d - y) + k_d(\dot{y}_d - \dot{y}) + k_i \int (y_d - y) dt \quad (2.6)$$

Where

k_p Proportional gain
 x_d Desired x position
 k_d Derivative gain
 \dot{x}_d Desired x position rate of change
 y_d Desired y position
 \dot{y}_d Desired y position rate of change
 k_i Integral gain

2-6 PID Controller Simulation

Genetic Algorithm was used to tune the PID controller gains with desired values and trajectories. There is no steady state error observed so in this case $k_i = 0$.

The system has been tested with and without disturbances. The disturbance (wind) was added in the form of additional forces and moments to the right side of the system's translational and rotational equations of motion (1.14) (1.4).

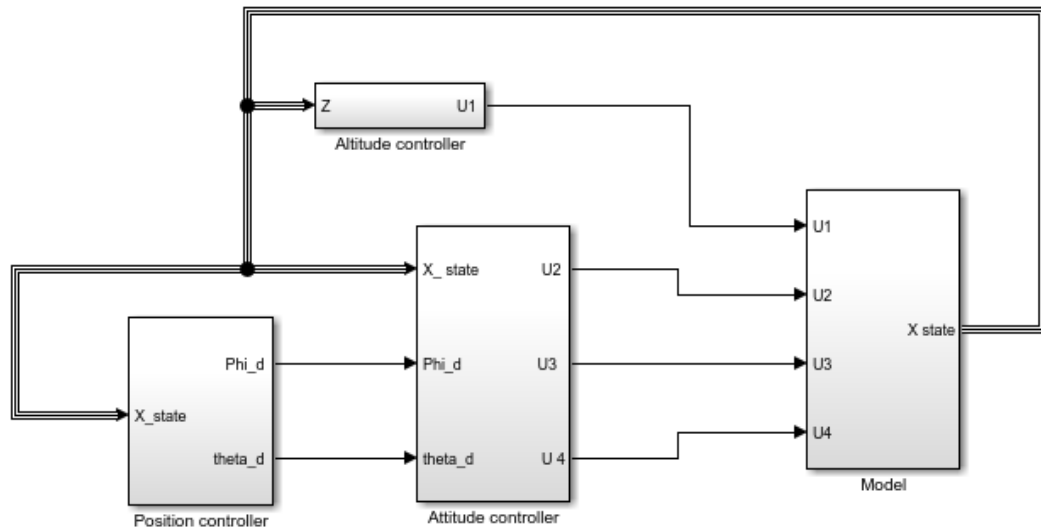


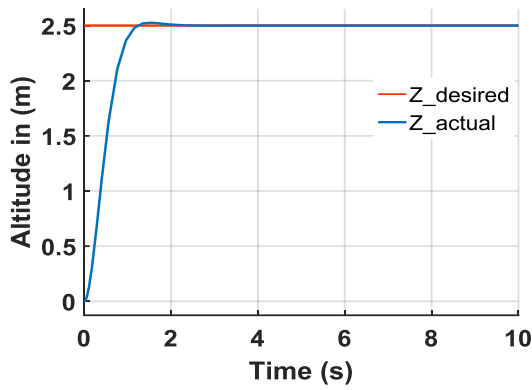
Fig. 2-2: Global View of the Simulink Model of the System with PD Control

Table 2.1: Tuning PD parameters

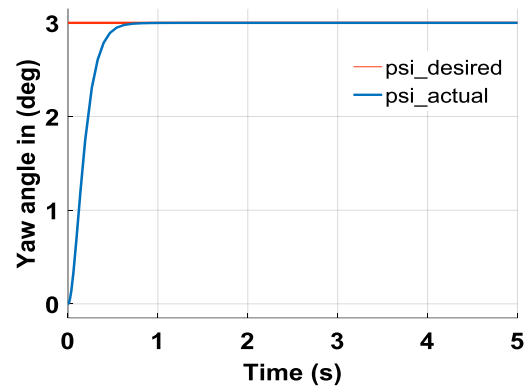
	Desired values	k_p	k_d	Settling time (s)	Over Shoot %
Altitude (z)	2.5	6.5	2.9	1.42	0.8
Attitude (ϕ and θ)	3	6.1	0.69	0.35	0.5
Heading (ψ)	3	4.5	0.82	0.68	0.5
Position (x and y)	3	1.3	0.81	2.4	2.57

2-6-1 PD Simulation without Disturbance

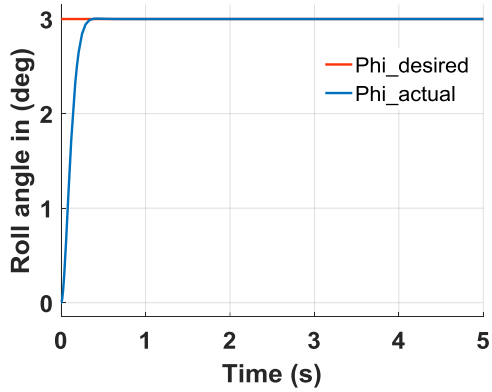
PD control is excellent and the tracking error is negligible. Fig. 2-3, 2-4, 2-5 represents the Altitude, Attitude, Heading, Position, controller inputs, and trajectory.



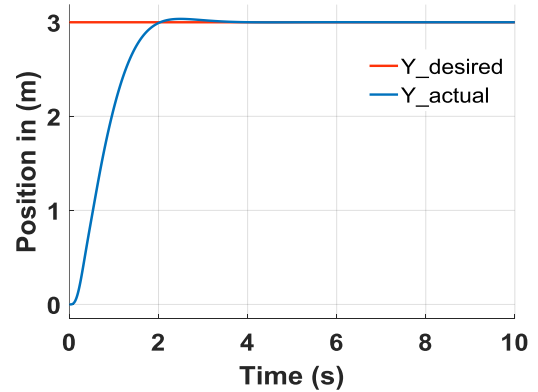
(a) Altitude Response



(b) Heading Response

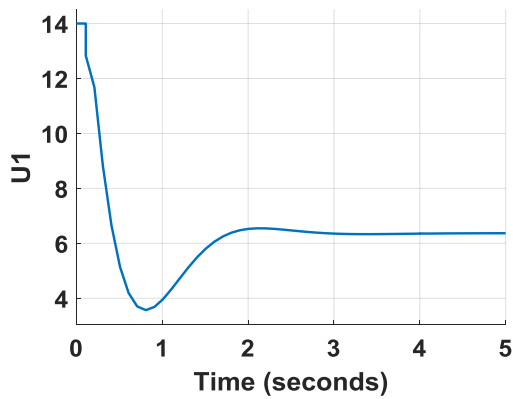


(c) Attitude Response

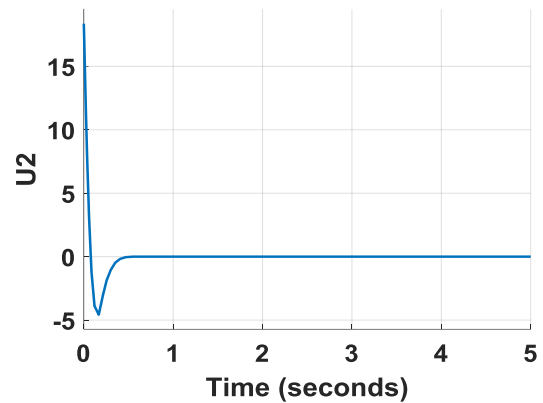


(d) Position Response

Fig.2-3: PD Controller Simulation Response



(a) Control input U1



(b) Control input U2

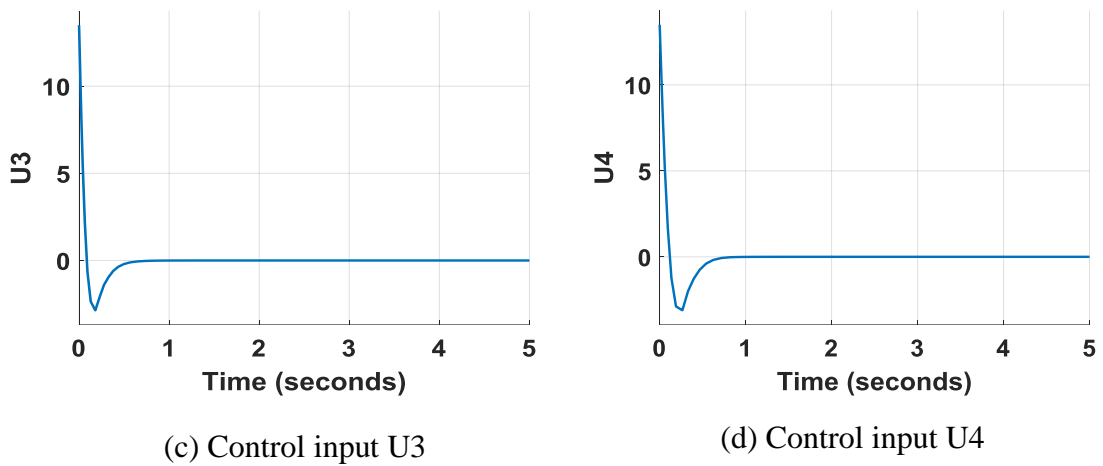


Fig. 2-4: PD Controllers

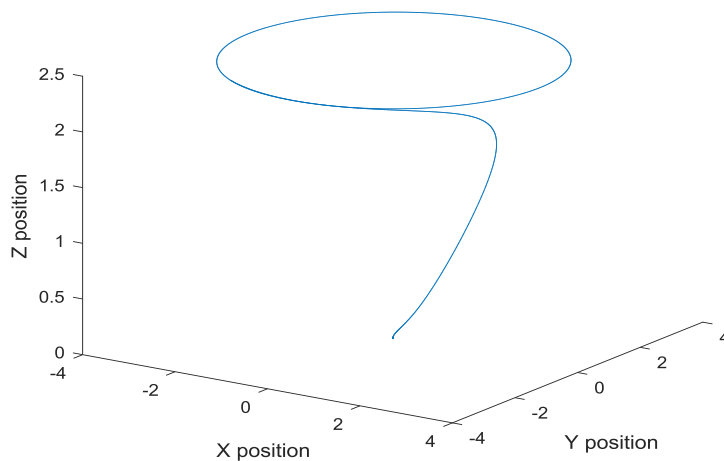
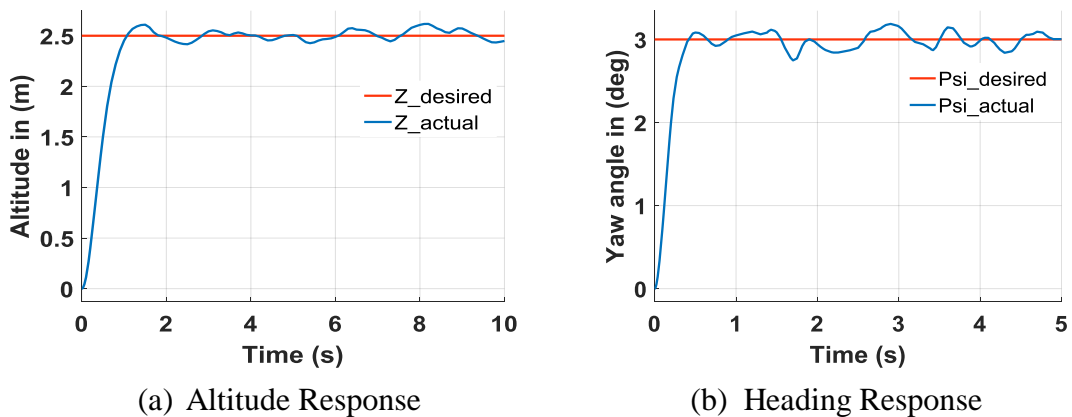
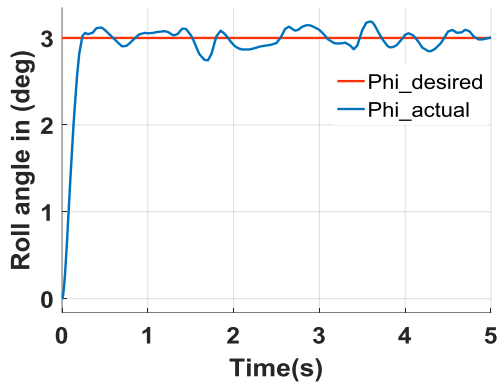


Fig. 2-5: Trajectory Response

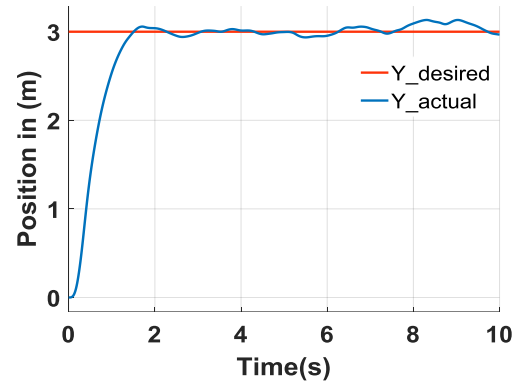
2-6-2 PD Simulation with Disturbance

Fig. 2-6, 2-7 show the Altitude, Attitude, Heading, Position, and controller inputs in the presence of disturbance.



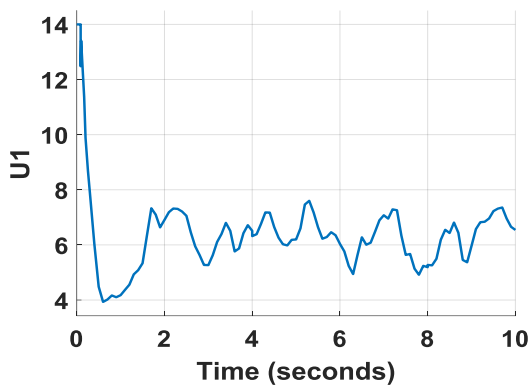


(c) Attitude Response

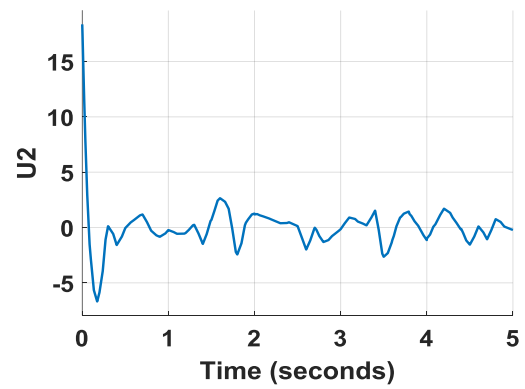


(d) Position Response

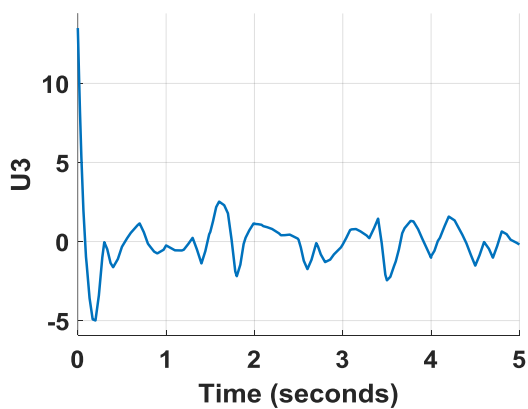
Fig. 2-6: PD Controller Simulation Response with Disturbance



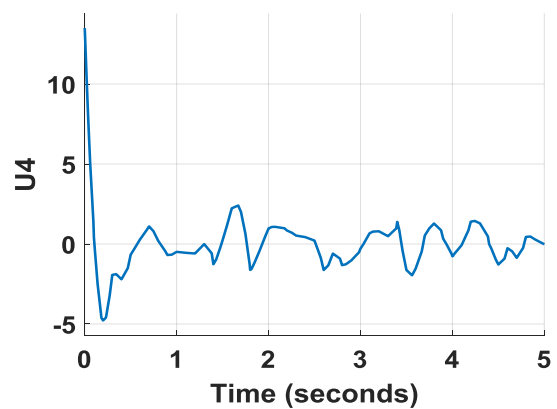
(a) Control Input U1



(b) Control Input U2



(c) Control Input U3



(d) Control Input U4

Fig. 2-7: PD Controllers with Disturbance

Chapter III Backstepping Controller

3-1 Backstepping Controller

In this chapter a Backstepping controller was developed to generate the desired control inputs for the quadrotor.

3-2 Introduction to Backstepping

Backstepping is control theory for a special class of nonlinear dynamic system, which is first developed by Petar v. Kokotovic and others in 1990. It is combined with Lyapunov control theory to make the closed-loop system with satisfied performance. The basic control principle of backstepping is that: firstly decompose the complex nonlinear system into several subsystems which are no more than the order of nonlinear system. And then design the Lyapunov function and virtual function for each subsystem. Because of the recursive structure, the control is able to be designed from the known-stable subsystem and « back out » new controller that progressively stabilize each outer subsystem. Finally, integrate all the controllers as the control law for the system.

3-3 Attitude and Heading Controller

The backstepping controller implemented to control the quadrotor's orientation is based on the control approaches proposed in [23] and [12].

3-3-1 Roll Controller

Extracting the two first states of the state space model in Equation (1.48) which are the roll angle and its rate of change, we get:

$$\dot{x}_1 = x_2 \quad (3.1)$$

$$\dot{x}_2 = x_4 x_6 a_1 - x_4 \Omega_r a_2 + b_1 U_2 \quad (3.2)$$

The roll angle subsystem is in the strict feedback form (only the last state is a function of the control input U_2) which makes it easy to pick a positive definite Lyapunov function for it.

$$V_1 = \frac{1}{2} z_1^2 \quad (3.3)$$

Where z_1 is the error between the desired and actual roll angle defined as follows.

$$z_1 = x_{1d} - x_1 \quad (3.4)$$

The time derivative of the Lyapunov function defined in Equation (3.3) is derived to be.

$$\dot{V}_1 = z_1 \dot{z}_1 \quad (3.5)$$

$$= z_1 (\dot{x}_{1d} - \dot{x}_1) \quad (3.6)$$

And from Equation (3.1) this can be written as,

$$\dot{V}_1 = z_1 (\dot{x}_{1d} - x_2) \quad (3.7)$$

According to Krasovskii-LaSalle principle, the system is guaranteed to be stable system if the time derivative of a positive definite Lyapunov function is negative semi definite [26]. To achieve that, we choose a positive definite bounding function. $W_1(z) = c_1 z_1^2$ to bound \dot{V}_1 as in Equation (3.8). This choice of $W_1(z)$ is also a common choice for a bounding function for strict feedback systems [26].

$$\dot{V}_1 = z_1 (\dot{x}_{1d} - x_2) \leq -c_1 z_1^2 \quad (3.8)$$

Where c_1 is a positive constant. To satisfy this inequality the virtual control input can be chosen to be,

$$(x_2)_{desired} = \dot{x}_{1d} + c_1 z_1 \quad (3.9)$$

Defining a new error variable z_2 to be the deviation of the state x_2 from its desired value,

$$z_2 = x_2 - \dot{x}_{1d} - c_1 z_1 \quad (3.10)$$

Substituting by the value of x_2 from the last equation in equation (3.7) we get,

$$\begin{aligned} \dot{V}_1 &= z_1 \dot{z}_1 \\ &= z_1 (\dot{x}_{1d} - x_2) \\ &= z_1 (\dot{x}_{1d} - (z_2 + \dot{x}_{1d} + c_1 z_1)) \\ &= -z_1 z_2 - c_1 z_1^2 \end{aligned} \quad (3.11)$$

The presence of the term $z_1 z_2$ in \dot{V}_1 may not lead to a negative semi-definite time derivative but this will be taken care of in the next iteration of the backstepping algorithm. The next step is to augment the first Lyapunov function V_1 with a quadratic term in the second error variable z_2 to get a positive definite V_2

$$V_2 = V_1 + \frac{1}{2} z_2^2 \quad (3.12)$$

With time derivative,

$$\begin{aligned} \dot{V}_2 &= \dot{V}_1 + z_2 \dot{z}_2 \\ &= -z_1 z_2 - c_1 z_1^2 + z_2(\dot{x}_2 - \ddot{x}_{1d} - c_1 \dot{z}_1) \end{aligned} \quad (3.13)$$

Choosing $W_2(z) = -c_1 z_1^2 - c_2 z_2^2$ to be the positive definite bounding function, with c_2 is positive constant and by replacing the value of \dot{x}_2 from equation (3.2) leads to the following inequality,

$$\dot{V}_2 = -z_1 z_2 - c_1 z_1^2 + z_2(x_4 x_6 a_1 - x_4 \Omega_r a_2 + b_1 U_2 - \ddot{x}_{1d} - c_1 \dot{z}_1) \leq -c_1 z_1^2 - c_2 z_2^2 \quad (3.14)$$

Simplifying the last inequality, the control input U_2 can be written as,

$$U_2 = \frac{1}{b_1} (-c_2 z_2 + z_1 - x_4 x_6 a_1 + x_4 \Omega_r a_2 + \ddot{x}_{1d} + c_1 \dot{x}_{1d} - c_1 x_2) \quad (3.15)$$

3-3-2 Pitch Controller

To derive the pitch controller we follow the same steps as we did before for the Roll controller, Extracting the third and the fourth states of the state space model in Equation (1.48) which are the pitch angle and its rate of change, we get:

$$\dot{x}_3 = x_4 \quad (3.16)$$

$$\dot{x}_4 = x_2 x_6 a_3 + x_2 \Omega_r a_4 + b_2 U_3 \quad (3.17)$$

And the error in pitch is defined as $z_3 = x_{3d} - x_3$ leading to a positive definite lyapunov function,

$$V_3 = \frac{1}{2} z_3^2 \quad (3.18)$$

With time derivative,

$$\begin{aligned} \dot{V}_3 &= z_3 \dot{z}_3 \\ &= z_3(\dot{x}_{3d} - x_4) \end{aligned} \quad (3.19)$$

Choosing $W_3(z) = -c_3 z_3^2$ to be the bounding function where c_3 a positive constant, the desired x_4 state is,

$$(x_4)_{desired} = \dot{x}_{3d} + c_3 z_3 \quad (3.20)$$

And the error in state x_4 is,

$$z_4 = x_4 - \dot{x}_{3d} - c_3 z_3 \quad (3.21)$$

Substituting by the value of x_4 from the last equation in equation (3.19) we get,

$$\begin{aligned} \dot{V}_3 &= z_3 \dot{z}_3 \\ &= z_3 (\dot{x}_{3d} - (z_4 + \dot{x}_{3d} + c_3 z_3)) \\ &= -z_3 z_4 - c_3 z_3^2 \end{aligned} \quad (3.22)$$

Augmenting the previous Lyapunov function with a quadratic term in the error variable z_4 ,

$$V_4 = V_3 + \frac{1}{2} z_4^2 \quad (3.23)$$

Defining a new bounding function to be $W_4(z) = -c_3 z_3^2 - c_4 z_4^2$ with c_4 a positive constant, the following inequality can be reached,

$$\dot{V}_4 = -z_3 z_4 - c_3 z_3^2 + z_4 (\dot{x}_4 - \ddot{x}_{3d} - c_3 z_3) \leq -c_3 z_3^2 - c_4 z_4^2 \quad (3.24)$$

Replacing x_4 with its definition from equation (3.17) and solving for U_3 . The roll angle control input is found to be,

$$U_3 = \frac{1}{b_2} (-c_4 z_4 + z_3 - x_2 x_6 a_3 - x_2 \Omega_r a_4 + \ddot{x}_{3d} + c_3 \dot{x}_{3d} - c_3 x_4) \quad (3.25)$$

3-3-3 Yaw Controller

Following exactly the same steps as the roll and pitch controllers, the control input for the yaw angle is derived to be,

$$U_4 = \frac{1}{b_3} (-c_6 z_6 + z_5 - x_2 x_4 a_5 + \ddot{x}_{5d} + c_5 \dot{x}_{5d} - c_5 x_6) \quad (3.26)$$

With

$$z_5 = x_{5d} - x_5 \quad (3.27)$$

$$z_6 = x_6 - \dot{x}_{5d} - c_5 z_5 \quad (3.28)$$

And c_5 and c_6 are positive constants.

3-4 Altitude Controller

For the altitude controller, the control input U_1 is derived in the same manner as $U_2, U_3, \text{ and } U_4$ to be

$$U_1 = \frac{m}{\cos x_1 \cos x_3} (z_7 + g - \ddot{x}_{7d} - c_7 \dot{x}_{7d} + c_7 x_8 - c_8 z_8) \tag{3.29}$$

With

$$z_7 = x_{7d} - x_7 \tag{3.30}$$

$$z_8 = x_8 - \dot{x}_{7d} - c_7 z_7 \tag{3.31}$$

And c_7 and c_8 are positive constants.

3-5 Backstepping Controller Simulation

Genetic Algorithm was used to tune the backstepping controller constants with desired values and trajectories. The system has been tested with and without disturbances. The disturbance (wind) was added in the form of additional forces and moments to the right side of the system’s translational and rotational equations of motion (1.14) (1.4).

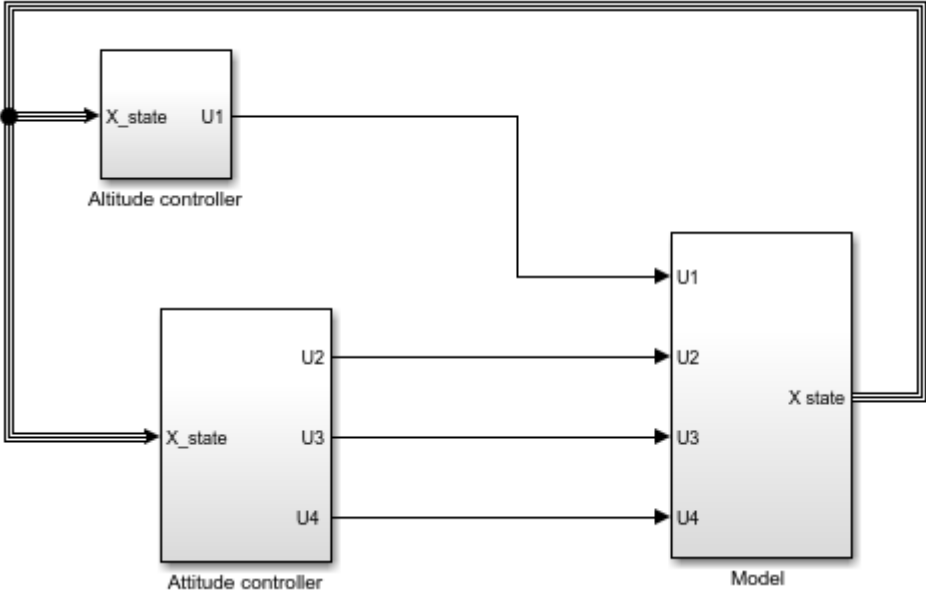


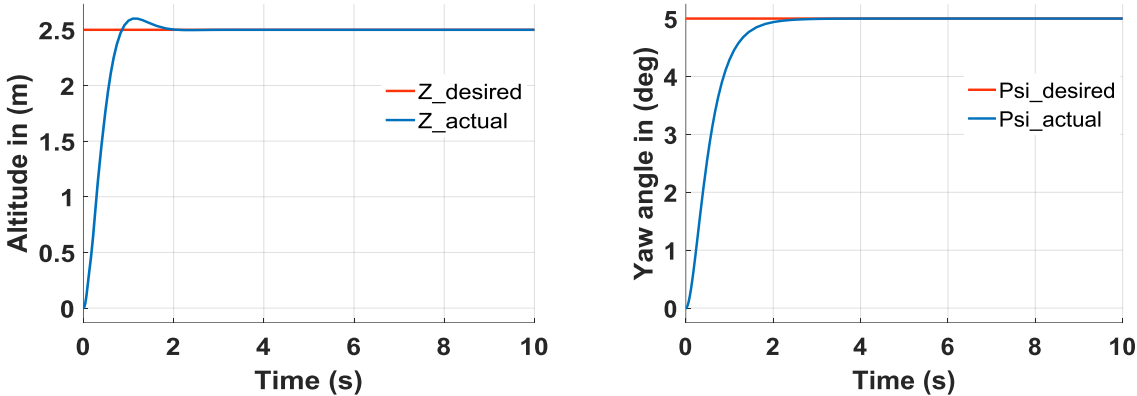
Fig. 3-1: Global view of the Simulink Model of the System with backstepping Control

Table 3.1: Tuning backstepping parameters

	Desired values	$C_7/C_1/ C_5$	$C_8/C_2/ C_4$	Settling time (s)	Over Shoot %
Altitude (z)	2.5	2.3	9.2	0.91	2.8
Attitude (ϕ and θ)	7	6.2	8.5	0.85	0.5
Heading (ψ)	5	4.5	2.5	1.62	0.5

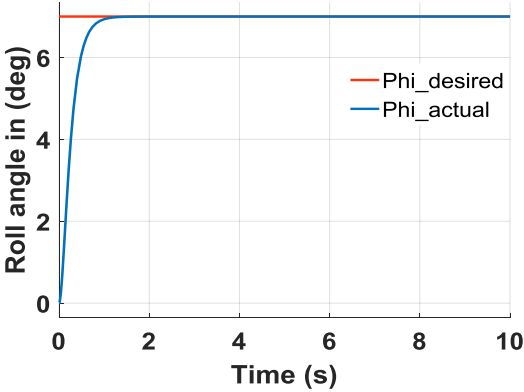
3-5-1 Backstepping Simulation without Disturbance

Without any disturbance, Backstepping control gives comparable results with proportional derivative. Fig. 3-2, 3-3, represents the Altitude, Attitude, Heading, and controller inputs.



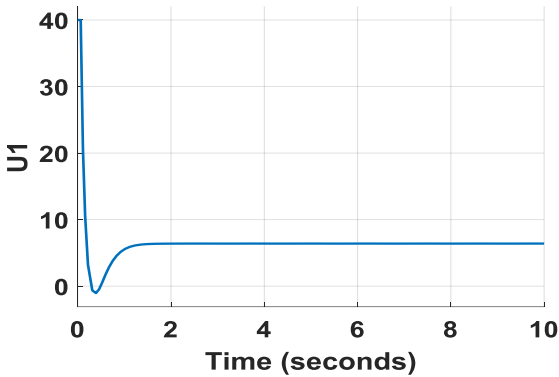
(a) Altitude Response

(b) Attitude Response

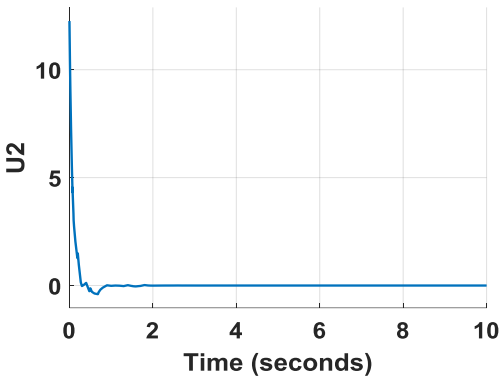


(c) Heading Response

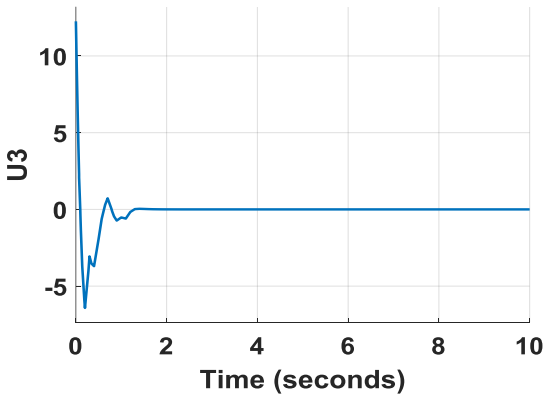
Fig. 3-2: Backstepping Controller Simulation Response



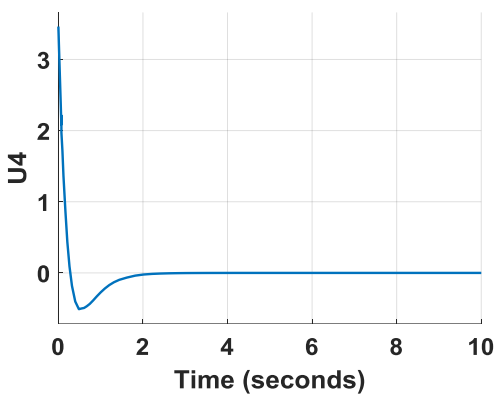
(a) Control Input U1



(b) Control Input U2



(c) Control Input U3

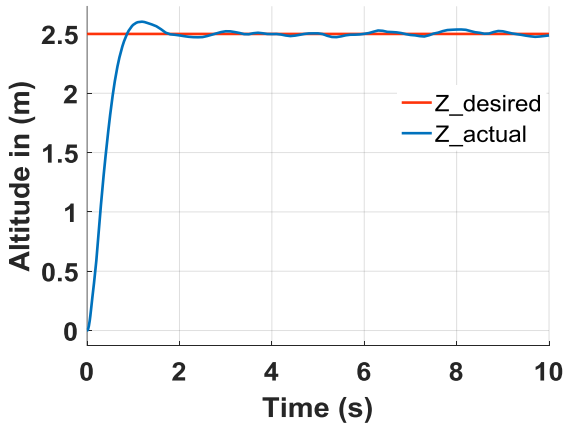


(d) Control Input U4

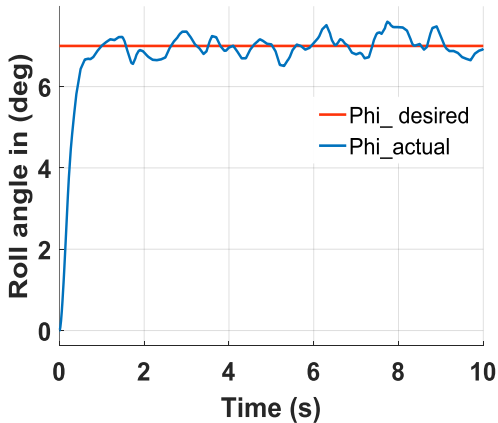
Fig. 3-3: Backstepping Controllers

3-5-2 Backstepping Simulation with Disturbance

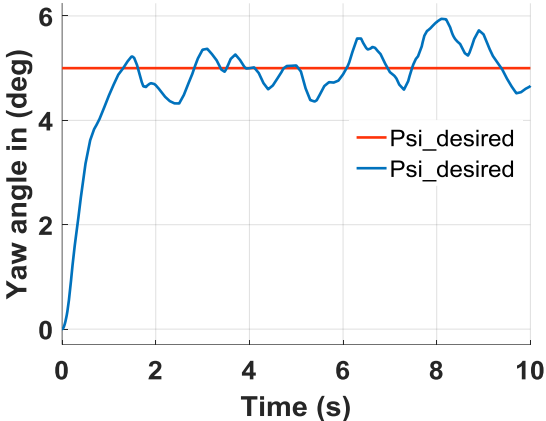
Fig. 3-4, 3-5 show the Altitude, Attitude, Heading, and controller inputs.in the presence of disturbance.



(a) Altitude Response

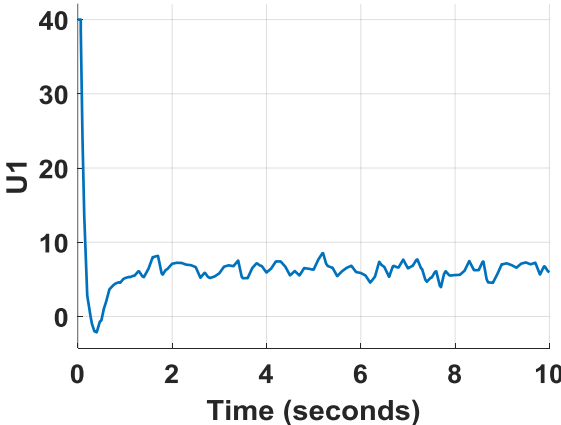


(b) Attitude Response

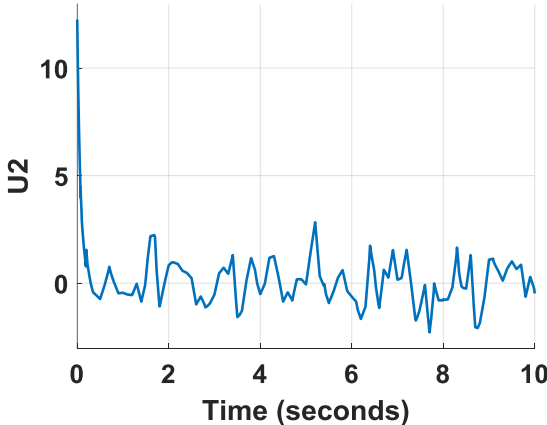


(c) Heading Response

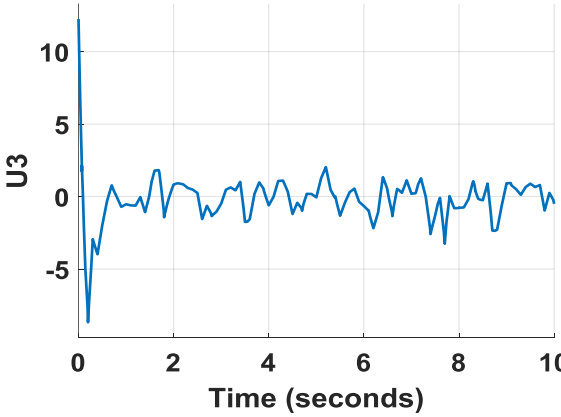
Fig. 3-4: Backstepping Controller Simulation Response with Disturbance



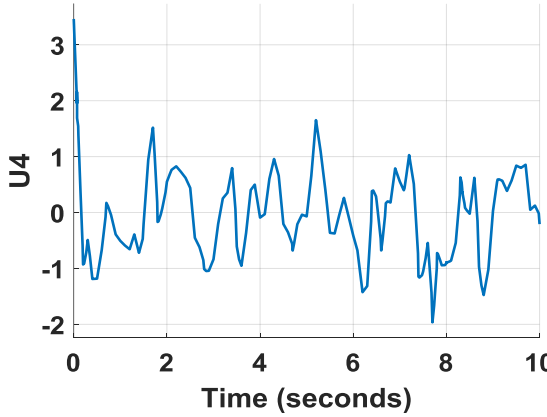
(a) Control Input U1



(b) Control Input U2



(c) Control Input U3



(d) Control Input U4

Fig. 3-5: Backstepping Controllers with Disturbance

Chapter IV Gain Scheduling Based PD Controller

4-1 Gain Scheduling Based PD Controller

In this chapter a Gain scheduling PD controller was developed to generates the desired control inputs for the quadrotor.

4-2 Introduction to Gain Scheduling

The theory behind gain scheduling is developing a set of controllers depending on the operating point of the system [27]. In this chapter, a family of PD controllers will be developed, each PD controller having different controller gains and will be able to stabilize the quadrotor system in certain range of operation. The acquired gains were used in a look up table, Fig. 4-1 shows the block diagram of developed gain scheduling based PD controller.

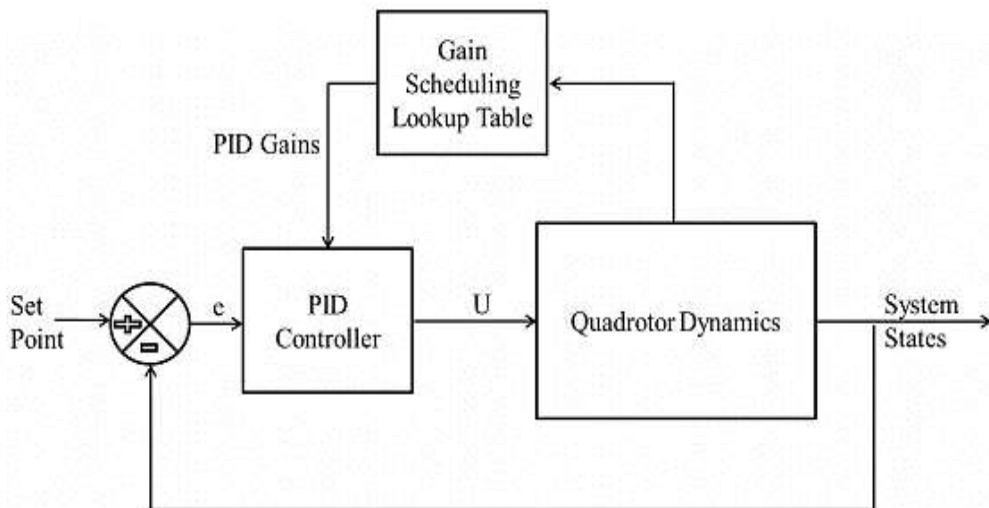


Fig. 4-1: Gain Scheduling Block Diagram

4-3 Gain Scheduling Based PD Controller Simulation

Genetic Algorithm was used to tune the PD controller gains for a desired set of operating points of altitude, attitude, and heading.

4-3-1 Altitude Controller

In this chapter we command the quadrotor to follow a varying trajectory to show the performance of the Gain Scheduling PD against the classical PD controller. Table 4-1 shows the tuned parameters of the PD controller for different desired altitudes. Figure 4-2 shows the comparison between the response of the Gain Scheduling PD and the classical PD.

Table 4-1: Altitude Gain Scheduling Based PD controller Gains

Desired Altitude	k_p	k_d	Settling Time (s)
1 m	8.60	3.41	1.02
2 m	6.21	3.19	1.41
3 m	5.09	2.80	1.47
4 m	5.57	3.11	1.53
5 m	5.35	2.90	1.43
6 m	6.25	3.11	1.42
7 m	5.61	2.85	1.49
8 m	5.96	3.15	1.58
9 m	5.08	2.77	1.66
10 m	5.74	3.23	1.76

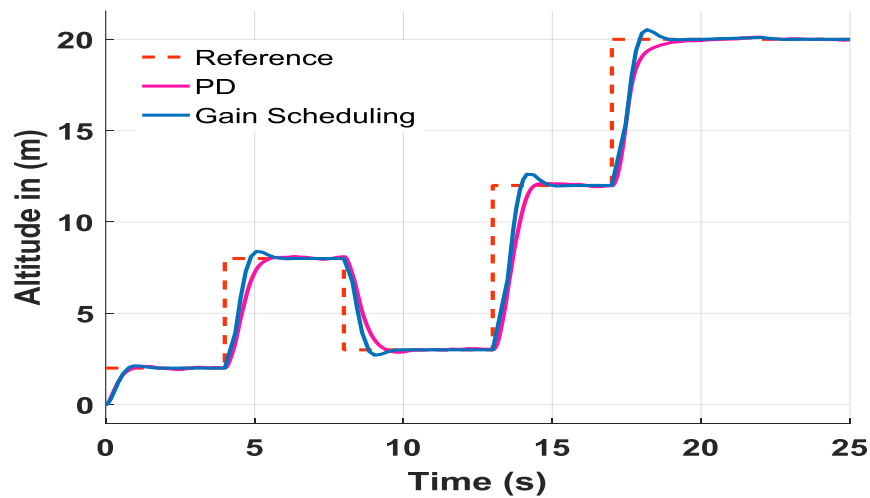


Fig. 4-3: Altitude Response

4-3-2 Attitude Controller

Table 4-2 shows the desired roll and pitch angles with their control gains and performance.

Figure 4-2 shows the comparison between the response of the Gain Scheduling PD and the classical PD in following a varying trajectory.

Table 4-2: Attitude Gain Scheduling Based PD controller Gains

Desired Attitude in (deg)	k_p	k_d	Settling Time (s)
2	6.53	0.711	0.31
4	5.72	0.682	0.35
6	6.81	0.772	0.37
8	6.63	0.784	0.44
10	5.18	0.619	0.41
12	5.74	0.710	0.45
14	5.79	0.718	0.48
16	4.69	0.611	0.48
18	3.70	0.513	0.49
20	5.07	0.634	0.47

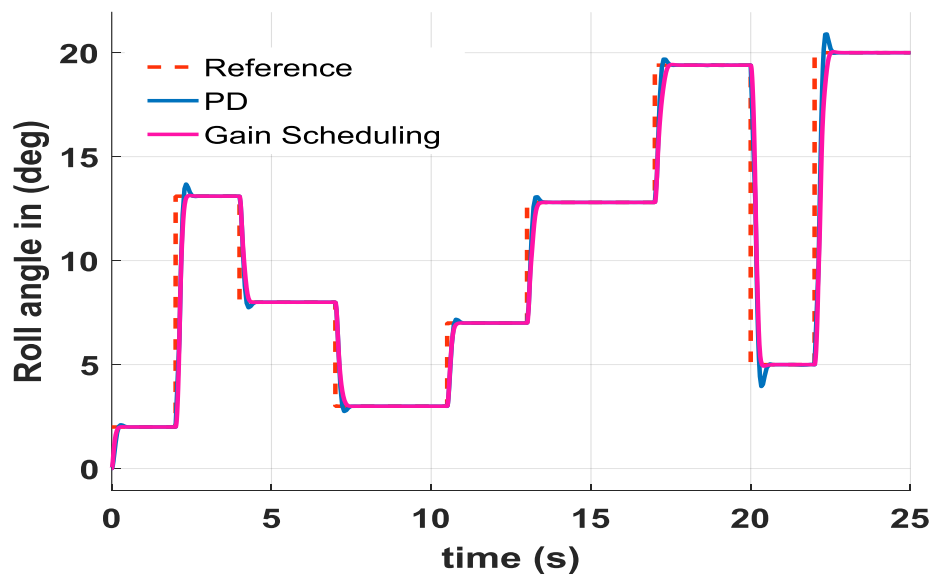


Fig. 4-3: Attitude Response

4-3-3 Heading Controller

The controller gains and their respective performances at multiple desired points are shown in table 4-3. and the response is shown in figure 4-4.

Table 4-3: Heading Gain Scheduling Based PD controller Gains

Desired Heading in (deg)	k_p	k_d	Settling Time (s)
2	6.81	0.985	0.42
4	3.49	0.771	0.71
6	5.21	0.803	0.45
8	3.42	0.651	0.63
10	4.12	0.792	0.67
12	3.88	0.799	0.76
14	4.32	0.885	0.81
16	3.12	0.717	0.89
18	3.42	0.862	0.93
20	4.31	0.992	0.96

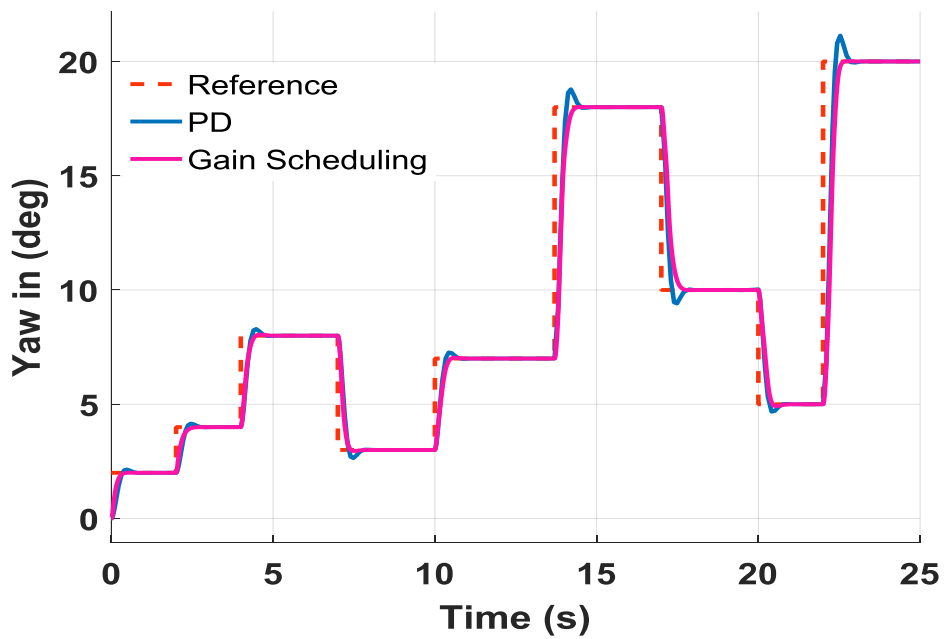
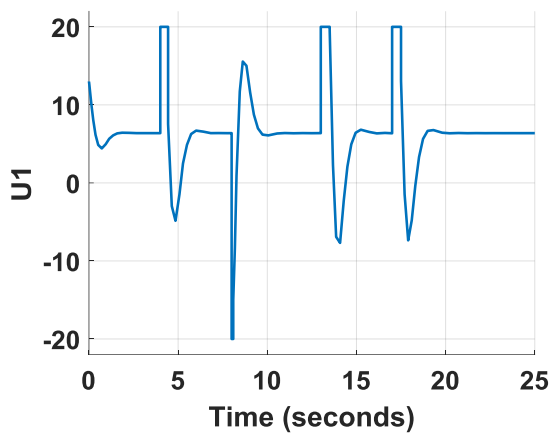
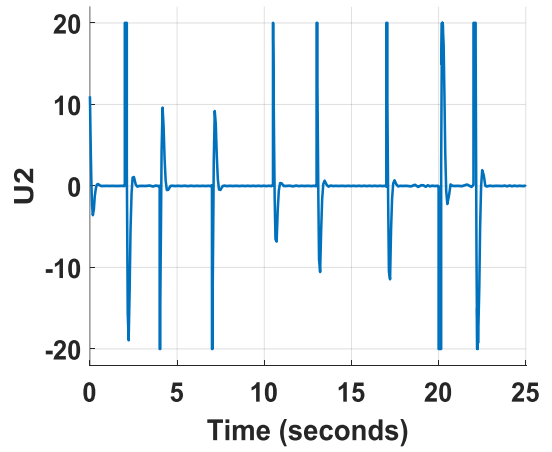


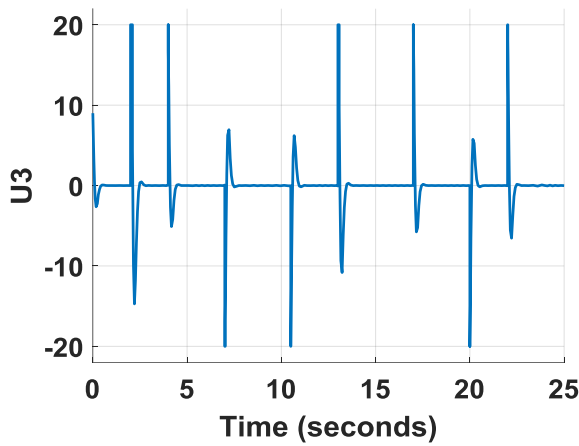
Fig. 4-4: Heading Response



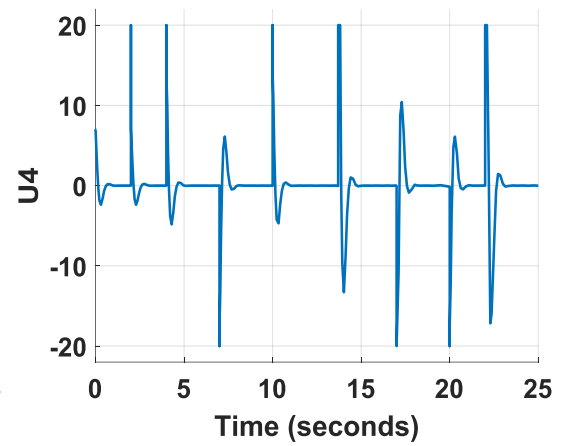
(a) Control Input U1



(b) Control Input U2



(c) Control Input U3



(d) Control Input U4

Fig. 4-5: Controller Inputs

4-4 Results Discussion

4-4-1 Proportional Derivative Control

The advantages of Proportional Derivative (PD) Control are :

- Tuning process is not complicated.
- Easy to understand and implement.
- Fewer tuning parameters.

Its disadvantages are :

- The control is not robust to disturbances and parameter variations.
- The derivative term creates problem in real systems. It amplifies the noise.

4-4-2 Backstepping Control

The advantages of Backstepping Control are :

- It does not involve cancelling of system non-linearities by feedback linearization, hence it is not system dependent.
- Ensure Lyapunov Stability.

Its disadvantages are :

- Several tuning parameters.
- The theory is mathematically exacting.

4-4-3 Gain Scheduling PD Control

The advantages of Gain Scheduling PD controller are :

- Adaptive to different operating conditions.
- Gives better performances in practical application of the quadrotor.

Its disadvantages are :

- The criticality of the switching time, the switching from a set of controller gains to the other has to be done in infinitesimally small time to guarantee a good performance.
- Several tuning parameters.

4-5 Comparison Between The Three Developed Controllers

Outside the linear region(away from hover), PD controller failed to stabilize the system due to its linear nature, and since the Gain Scheduling PD controller based on the linear PD controller,this last face the same problem in stabilizing the system, on the Other hand the Backstepping controller is able to stabilize the system with a good dynamic performance.

In the linear region(near hover), the three developed controllers give comparable dynamic performances.

When operating in a windy environement, PD and Backstepping controllers are comparable in controlling the altitude, but Backstepping suffered a slight performance degradation in stabilizing the quadrotor's attitude.

Comparing the three developed controllers in terms of their generated control signals U_1 through U_4 , PD comes out to be the most energy efficient followed by backstepping.Gain Scheduling PD suffer from spikes in the control signals due to the sudden transition between one set of control gains to the other.

General Conclusion

The purpose of this work was to derive a mathematical model for the quadrotor, and develop three linear and nonlinear control techniques ; a linear (Proportional-Derivative PD), a Gain Scheduling based PD controller, a nonlinear Backstepping controller to stabilize the states of the quadrotor. A complete simulation was then implemented on MATLAB/Simulink relying on the derived mathematical model of the quadrotor. The tuning of the parameters of the three used controllers is done using genetic algorithm GA. The Gain scheduling PD controller gave a better performance than the classical PD controller when the quadrotor was commanded to follow a varying trajectory, which is a more realistic application for a quadrotor UAV. The backstepping controller gave better performance outside the linear region due to its nonlinear nature. The PD and Backstepping controllers gave better performances in a windy environment. And the three controllers performed comparably in near hovering operation of the quadrotor.

Future Work

one valuable addition would be the robustification of the developed control techniques against wind as this is a common problem with quadrotors control and our simulation results showed a huge degradation of the performance of the controllers when the system is exposed to wind. Moreover, in our work it is assumed that all the model parameters are known accurately without any uncertainties, which is not the case in reality, thus, developing adaptive control algorithms to count for the system uncertainties would enhance the performance of the quadrotor when operating in a real environment. Adding an integral action to the developed Backstepping controller will lead to the formulation of an adaptive control algorithm robust to system uncertainties.

Appendix

Quadrotor Parameters

This appendix contains the quadrotor parameters used in the simulations. These parameters are adopted from Bouabdallah's thesis [25]

Parameter	Description	Value	unit
I_{xx}	MOI about body frame's x-axis	7.5e-3	kg.m ²
I_{yy}	MOI about body frame's y-axis	7.5e-3	kg.m ²
I_{zz}	MOI about body frame's z-axis	1.3e-2	kg.m ²
l	Moment arm	0.23	m
J_r	Rotor inertia	6e-5	kg.m ²
m	Quadrotor mass	0.650	kg
K_f	Aerodynamic force constant	3.13e-5	N s ²
K_M	Aerodynamic moment constant	7.5e-7	Nm s ²
R_{mot}	Motor circuit resistance	0.6	Ω
K_{mot}	Motor torque constant	5.2	mNm/A
K_t	Aerodynamic translation coefficient	diag(0.1, 0.1, 0.15)	Ns/m
K_t	Aerodynamic rotation coefficient	diag(0.1, 0.1, 0.15)	Nm s

Fig 5 : Quadrotor Parameters and Constants

Bibliography:

- [1].Anežka Chovancová, *Procedia Engineering*, “Mathematical Modelling and Parameter Identification of Quadrotor”, 96(2014) 172 – 181.
- [2].Pengcheng Wang, *IEEE*, 978-1-5090-5346, “Dynamics Modelling and Linear Control of Quadcopter”, 2016.
- [3]. Petar Piljek, *IEEE*, 14(1), “Mathematical Modelling Of Unmanned Aerial Vehicles With Four Rotors”, 88-100, 2016.
- [4].Hongning Hou, Jian Zhuang, Hu Xia, Guanwei Wang, and Dehong Yu. A simple controller of minisize quad-rotor vehicle. In *Mechatronics and Automation (ICMA), 2010 International Conference on*, pages 1701–1706, 2010. doi: 10.1109/ICMA.2010.5588802
- [5].Jinhyun Kim, Min-Sung Kang, and Sangdeok Park. Accurate modeling and robust hovering control for a quadrotor vtol aircraft. *Journal of Intelligent and Robotic Systems*, 57(1-4):9–26, 2010. ISSN 0921-0296. doi: 10.1007/s10846-009-9369-z. URL <http://dx.doi.org/10.1007/s10846-009-9369-z>.
- [6].Farid Kendoul. Survey of advances in guidance, navigation, and control of unmanned rotorcraft systems. *Journal of Field Robotics*, 29(2):315–378, 2012
- [7].Mark Willis Bailey. Unmanned aerial vehicle path planning and image processing for orthoimagery and digital surface model generation. 2012.
- [8].A. Azzam and Xinhua Wang. Quad rotor arial robot dynamic modeling and configuration stabilization. In *Informatics in Control, Automation and Robotics (CAR), 2010 2nd International Asia Conference on*, volume 1, pages 438–444, 2010. doi: 10.1109/CAR.2010.5456804.
- [9].S. Bouabdallah, A. Noth, and R. Siegwart. PID vs LQ control techniques applied to an indoor micro quadrotor. In *Intelligent Robots and Systems, 2004. (IROS 2004). Proceedings. 2004 IEEE/RSJ International Conference on*, volume 3, pages 2451–2456 vol.3, 2004. doi: 10.1109/IROS.2004.1389776.
- [10]. V. Mistler, A. Benallegue, and N.K. M’Sirdi. Exact linearization and noninteracting control of a 4 rotors helicopter via dynamic feedback. In *Robot and Human Interactive Communication, 2001. Proceedings. 10th IEEE International Workshop on*, pages 586–593, 2001. doi: 10.1109/ROMAN.2001.981968.
- [11].Jun Li and Yuntang Li. Dynamic analysis and PID control for a quadrotor. In *Mechatronics and Automation (ICMA), 2011 International Conference on*, pages 573–578, 2011. doi: 10.1109/ICMA.2011.5985724.

- [12]. S. Bouabdallah and R. Siegwart. Backstepping and sliding-mode techniques applied to an indoor micro quadrotor. In *Robotics and Automation, 2005. ICRA 2005. Proceedings of the 2005 IEEE International Conference on*, pages 2247–2252, 2005. doi: 10.1109/ROBOT.2005.1570447.
- [13]. Samir Bouabdallah. *Design and control of quadrotors with application to autonomous flying*. Phd. thesis, Ecole Polytechnique Federale de Lausanne, 2007.
- [14]. Paul Edward Ian Pounds. *Design, construction and control of a large quadrotor micro air vehicle*. Phd. thesis, Australian National University, 2007.
- [15]. S. Bouabdallah, A. Noth, and R. Siegwart. PID vs LQ control techniques applied to an indoor micro quadrotor. In *Intelligent Robots and Systems, 2004. (IROS 2004). Proceedings. 2004 IEEE/RSJ International Conference on*, volume 3, pages 2451–2456 vol.3, 2004. doi: 10.1109/IROS.2004.1389776.
- [16]. Jinpeng Yang, Zhihao Cai, Qing Lin, and Yingxun Wang. Self-tuning pid control design for quadrotor uav based on adaptive pole placement control. In *Chinese Automation Congress (CAC), 2013*, pages 233–237. IEEE, 2013
- [17]. Guilherme V Raffo, Manuel G Ortega, and Francisco R Rubio. An integral predictive/nonlinear h control structure for a quadrotor helicopter. *Automatica*, 46(1):29–39, 2010
- [18]. Gergely Regula. *Formation control of autonomous aerial vehicles*. Phd thesis, Budapest University of Tech G. M. H. H. M. P. V. a. C. J. T. Jeremy H Gillula, “Applications of hybrid reachability analysis to robotic aerial vehicles,” *The International Journal of Robotics Research*, 30(3):335–354, 2011. nology and Economics, 2013
- [19]. H. T. R. I. M. A. H. P. A. C. a. Y. Y. A. Ataka, “Controllability and observability analysis of the gain scheduling based linearization for uav quadrotor,” In *Robotics, Biomimetics, and Intelligent Computational Systems (ROBIONETICS), 2013 IEEE International Conference on*, pages 212–218, Nov 2013. doi: 10.1109/ROBIONETICS.2013.6743606.
- [20]. A. C. a. Y. Z. Mohammad Hadi Amoozgar, “Fault tolerant fuzzy gain scheduled pid for a quadrotor helicopter testbed in the presence of actuator faults,” In *IFAC Conference on Advances in PID Control, Brescia, Italy (March 2012)*, 2012.
- [21]. M. A. a. Y. M. Z. Iman Sadeghzadeh, “payload drop application of unmanned quadrotor helicopter using gain-scheduled pid and model predictive control techniques,” In *Intelligent Robotics and Applications*, pages 386–395. Springer, 2012..
- [22] T. Madani and A. Benallegue. Backstepping control for a quadrotor helicopter. In *Intelligent Robots and Systems, 2006 IEEE/RSJ International Conference on*, pages 3255–3260, 2006. doi: 10.1109/IROS.2006.282433.

- [23]. Amr Nagaty, Sajad Saeedi, Carl Thibault, Mae Seto, and Howard Li. Control and navigation framework for quadrotor helicopters. *Journal of Intelligent and Robotic Systems*, 70(1-4):1–12, 2013. ISSN 0921-0296. doi: 10.1007/s10846-012-9789-z. URL <http://dx.doi.org/10.1007/s10846-012-9789-z>.
- [24]. L Derafa, T Madani, and A Benallegue. Dynamic modelling and experimental identification of four rotors helicopter parameters. In *Industrial Technology, 2006. ICIT 2006. IEEE International Conference on*, pages 1834–1839. IEEE, 2006.
- [25]. Samir BOUABDALLAH, “design and control of quadrotors with application to autonomous flying,” in *THÈSE NO 3727 (2007), à LA FACULTÉ DES SCIENCES ET TECHNIQUES DE L'INGÉNIEUR*.
- [26]. Miroslav Krstic, Petar V Kokotovic, and Ioannis Kanellakopoulos. *Nonlinear and adaptive control design*. John Wiley & Sons, Inc., 1995.
- [27]. Kenneth H McNichols and M Sami Fadali. Selecting operating points for discrete time gain scheduling. *Computers & Electrical Engineering*, 29(2):289-301, 2003.